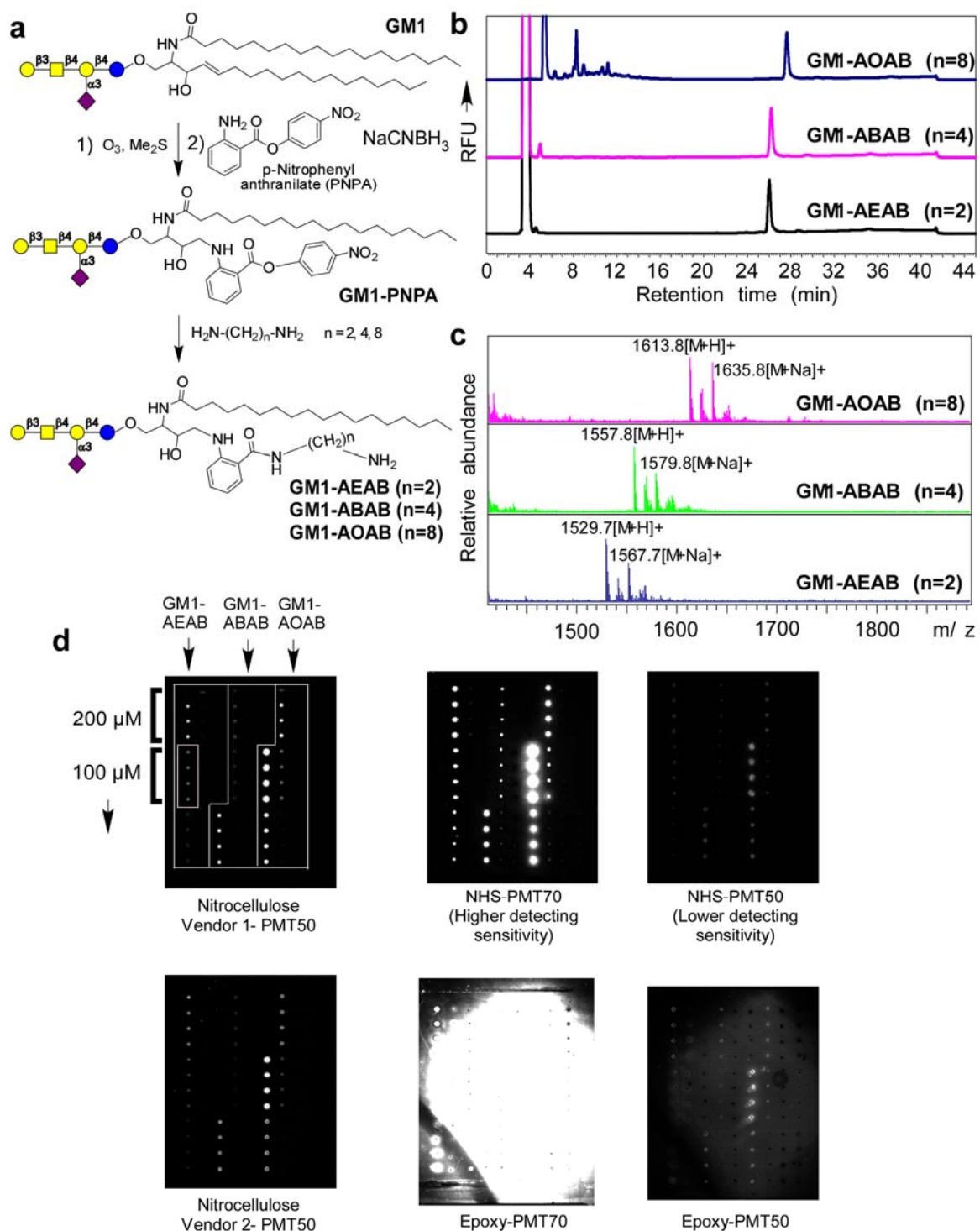
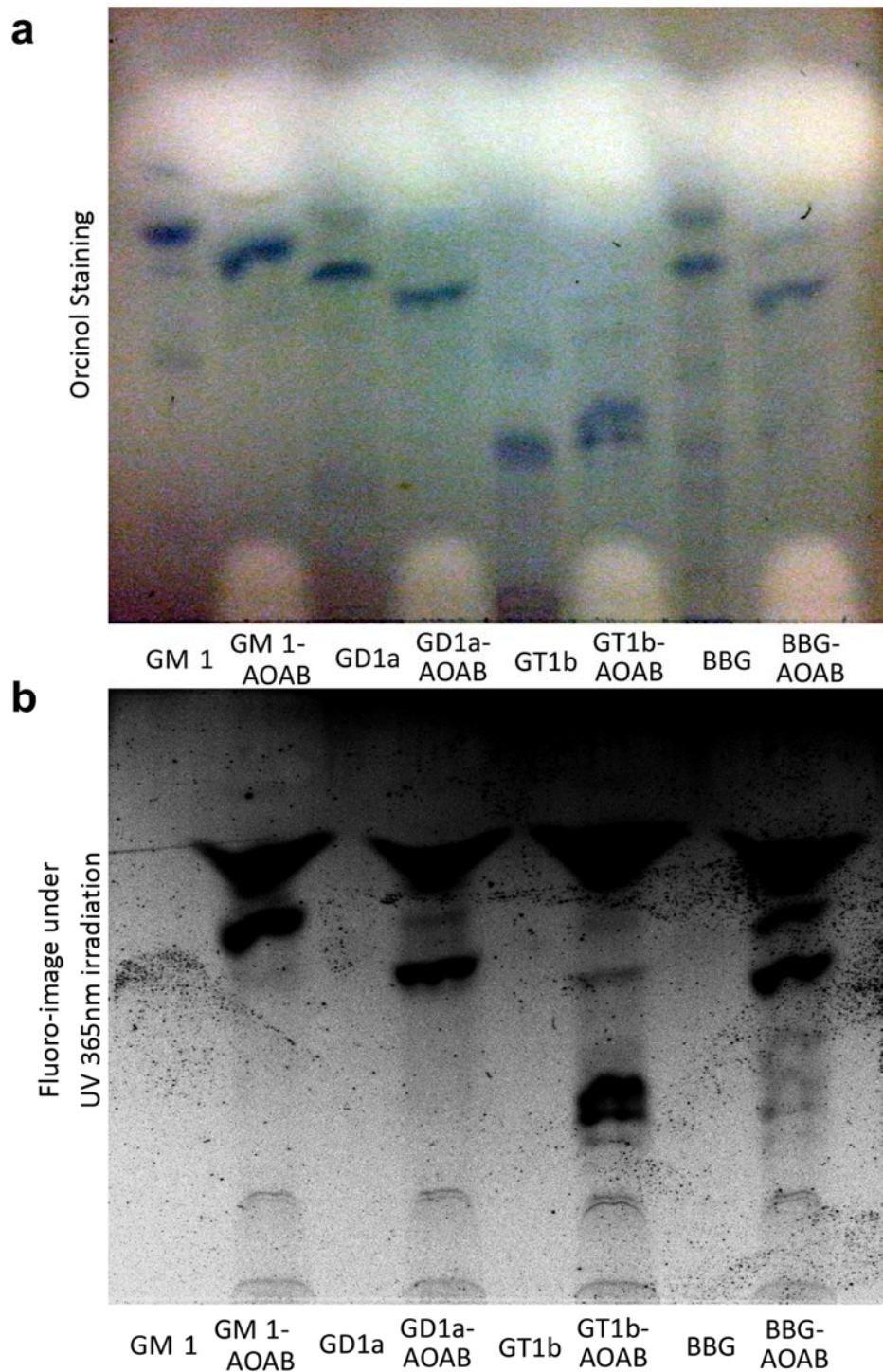


Supplementary Data

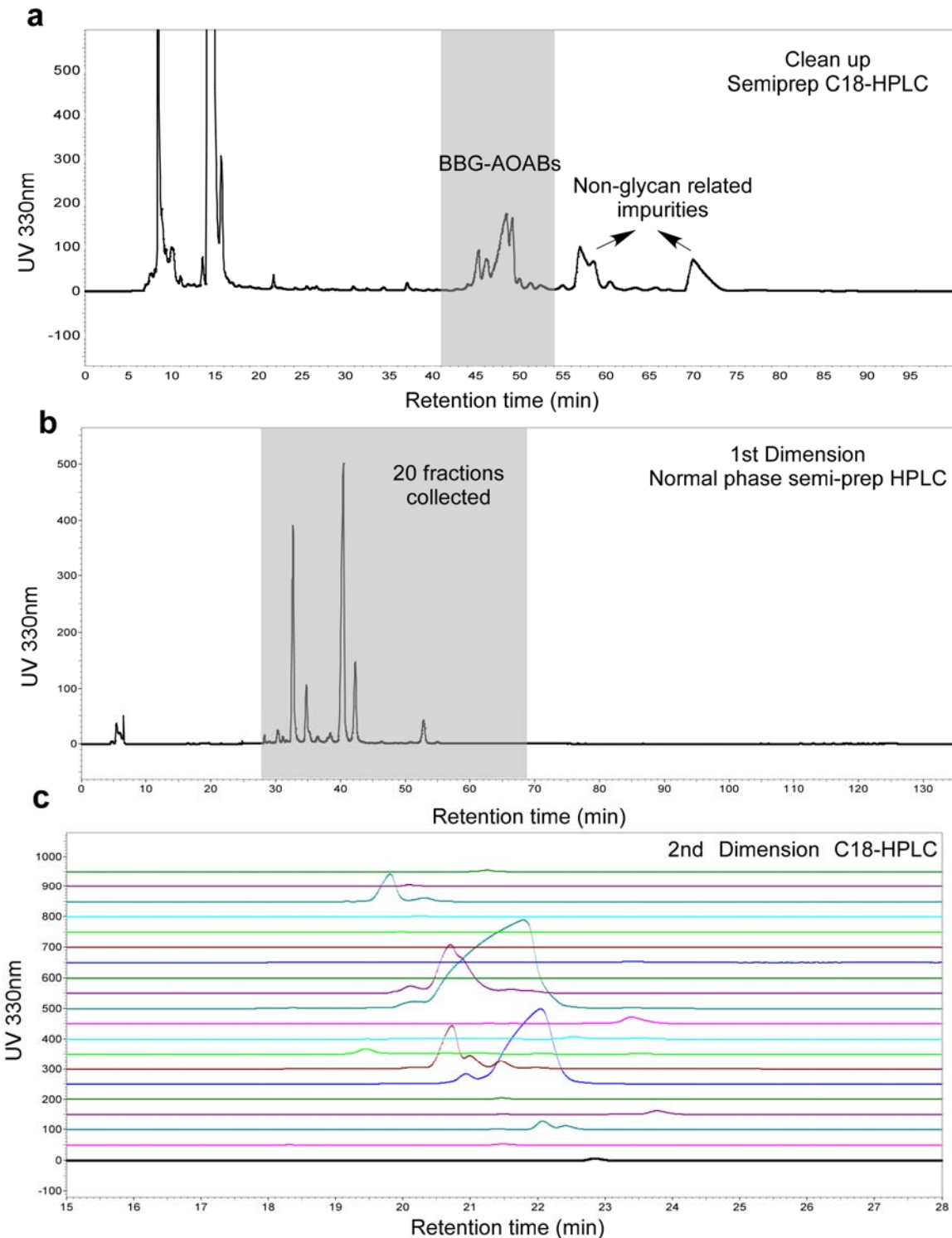


Supplementary Figure 1. The bifunctional fluorescent derivatization of glycosphingolipids and the validation of microarray printing. **(a)** The monosialyl ganglioside GM1 (Gal β 1-3GalNAc β 1-4(Neu5Aco2-3)Gal β 1-4Glc β 1-ceramide) is treated with ozone, PNPA, and diamines with different lengths. Treatment of PNPA conjugates with ethylenediamine yielded AEAB

conjugates, while treatment with 1,4-diaminobutane and 1,8-diaminoctane (ODA) generated homologs with varied lengths, termed N-(aminobutyl)-2-amino benzamide (ABAB) and N-(aminoctyl)-2-amino benzamide (AOAB) conjugates. The fluorescent GM1 conjugates are named as GM1-AEAB, GM1-ABAB and GM1-AOAB; **(b)** C18-HPLC profiles of GM1-AEAB, GM1-ABAB and GM1-AOAB; all products gave a single fluorescent product peak by C18-HPLC; **(c)** MALDI-TOF profiles of GM1-AEAB, GM1-ABAB and GM1-AOAB, showing masses matching calculated values. **(d)** The test printing of GM1-AEAB, GM1-ABAB and GM1-AOAB at different concentrations. The three GM1 derivatives were quantified based on fluorescence, printed on three different glass slides, and interrogated with biotinylated cholera toxin subunit B (CTSB), which specifically binds the GM1 glycan. They were printed on 4 slides: nitrocellulose-vendor 1, nitrocellulose-vendor 2, NHS and epoxy slides. For each sample, 8 concentrations (200, 100, 50, 25, 12.5, 6.25, 3.13, 1.6 μ M) were printed in replicates of n = 4 for each concentration. The slides were interrogated with biotinylated CTSB and detected by cyanine5-streptavidin. The slides were scanned at different photomultiplier tube (PMT) settings. PMT 70 has higher detecting sensitivity than PMT 50. For nitrocellulose slides, lower PMT (50) had to be used due to the autofluorescence of nitrocellulose membrane. For glass slides, either NHS or epoxy, higher PMT (70) was used to reach a higher sensitivity. When background is high (such as the epoxy slide in the following picture), lower PMT (50) can be used to reduce the background. The pictures show the fluorescent images on different slides and their brightness/contrast ratio have been adjusted. The comparative studies by printing of the three GM1 derivatives on nitrocellulose slides and NHS- or epoxy-slides demonstrate that the N-(aminoctyl)-2-amino benzamide (AOAB) conjugates, GM1-AOAB with the C₈ extension was detected by CTSB with greater sensitivity than the other derivatives. The longer alkyl chain of GM1-AOAB, which increases its hydrophobicity, may increase the printing efficiency or, more possibly, may help to organize the parallel fatty acid chain, reducing its interference between binding of CTSB and glycan.

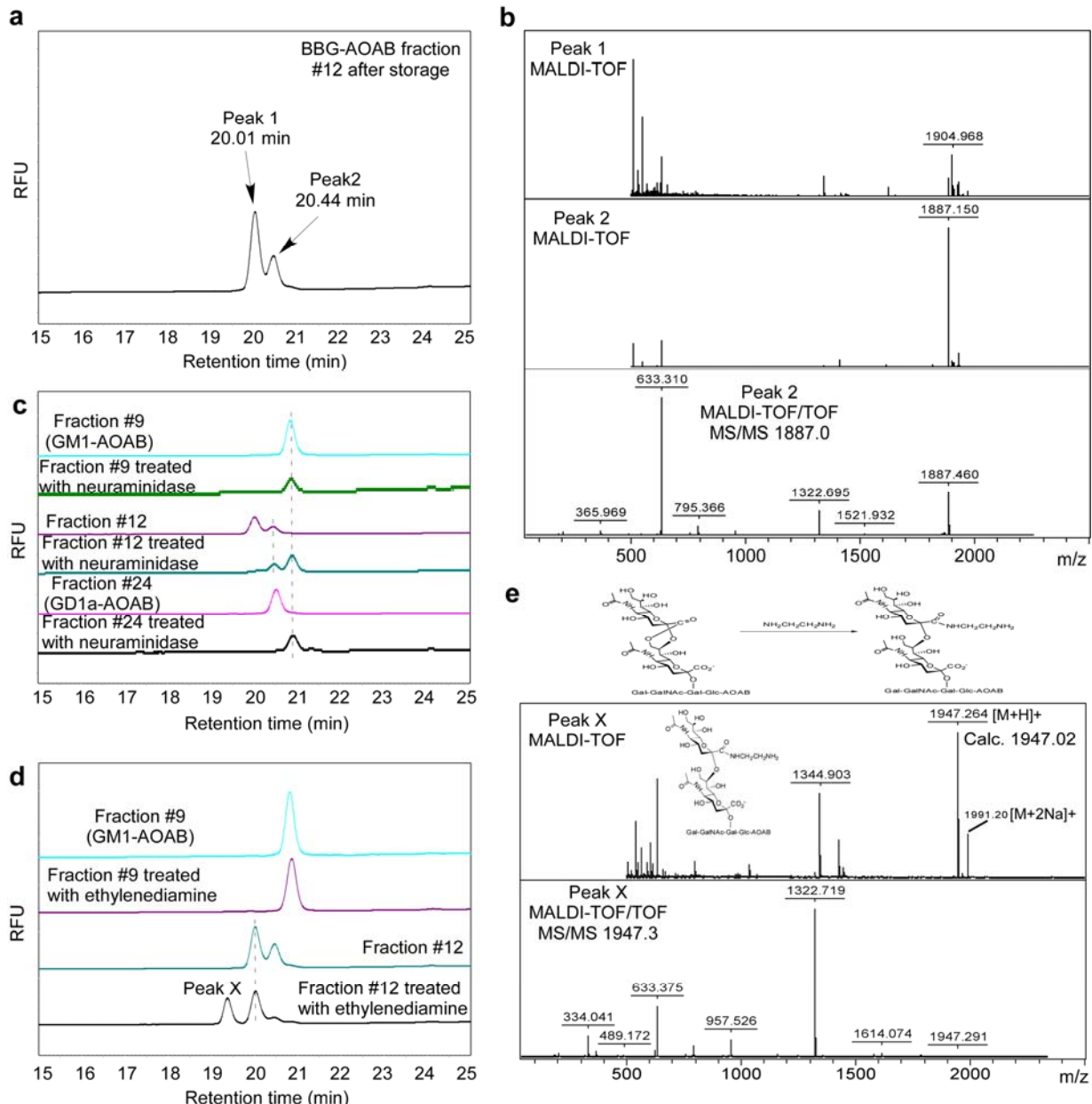


Supplementary Figure 2. Thin-layer chromatography (TLC) image of GM1, GD1a, GT1b, BBG, and their corresponding AOAB conjugates by orcinol staining (**a**) or fluorescence upon UV irradiation (**b**).



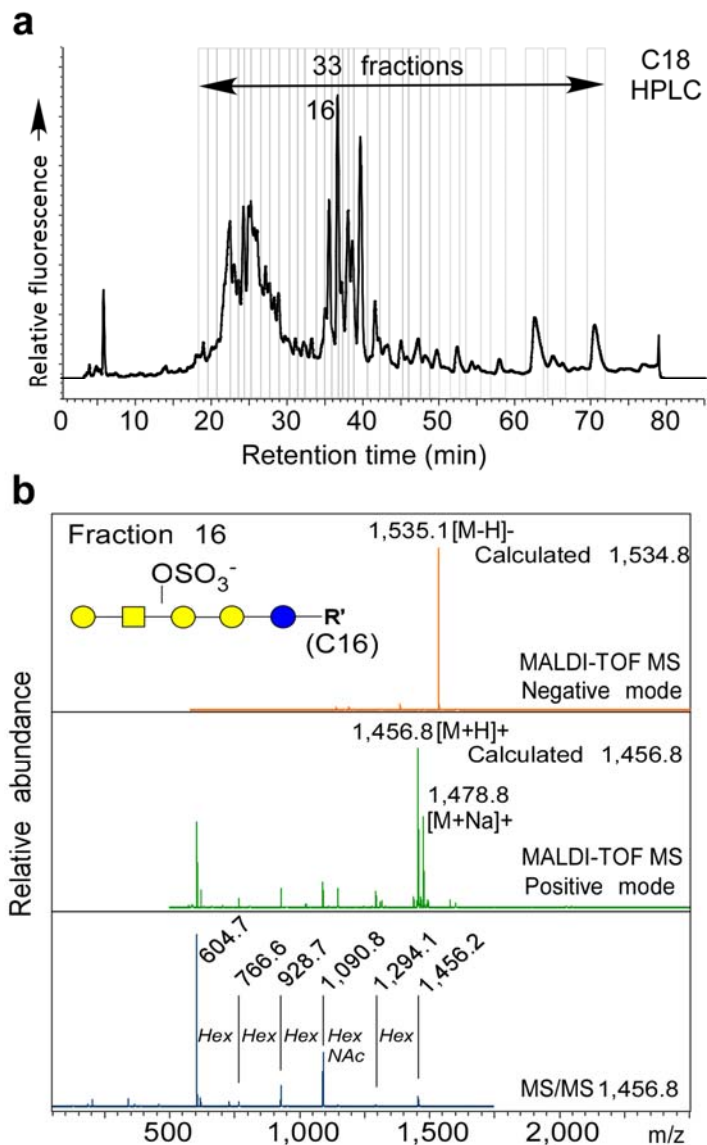
Supplementary Figure 3. The 2D HPLC separation of BBG GSL-AOABs. Bovine brain gangliosides were treated with ozone, quenched with methyl sulfide, dried over nitrogen and conjugated with PNPA. The mixture was precipitated with 10-20 volumes of water, centrifuged and filtered through a 0.2 µm membrane. The precipitate, unreacted PNPA, was discarded. The filtrate was lyophilized and treated with 1,8-diaminoctane, dried, neutralized with acetic acid. **(a)** The crude product was injected onto a C18 semi-prep HPLC column and eluent from 41-54

minutes (the gray area) was pooled as the fluorescently labeled glycolipids fractions. A Vydac C18 column (250 mm x 9.2 mm) was used. The mobile phase was acetonitrile and water with 0.1% trifluoroacetic acid (TFA). The flow rate was 2.5 ml min⁻¹. The concentration of acetonitrile increased from 15% to 90% linearly over 75 minutes. **(b)** The pooled eluent was dried, lyophilized, reconstituted in methanol, and injected into normal phase semi-preparative HPLC for 1st dimension separation; 20 fractions were collected. **(c)** All normal phase fractions were briefly evaporated in Speed-vac to remove organic solvent and then lyophilized. The lyophilized material was reconstituted in water and separated on a C18 reverse phase HPLC column. Fractions were collected manually as peaks. The HPLC profiles (retention time 15 to 28 minutes) of the second dimension C18 HPLC separation of the normal fractions are shown below (from bottom to top: normal phase fraction #1 to #20). Fractions were rechromatographed on the same C18 HPLC column with a different gradient to check the homogeneity and further separate glycans if several peaks were present. A total of 40 fractions were obtained in the tagged ganglioside library.

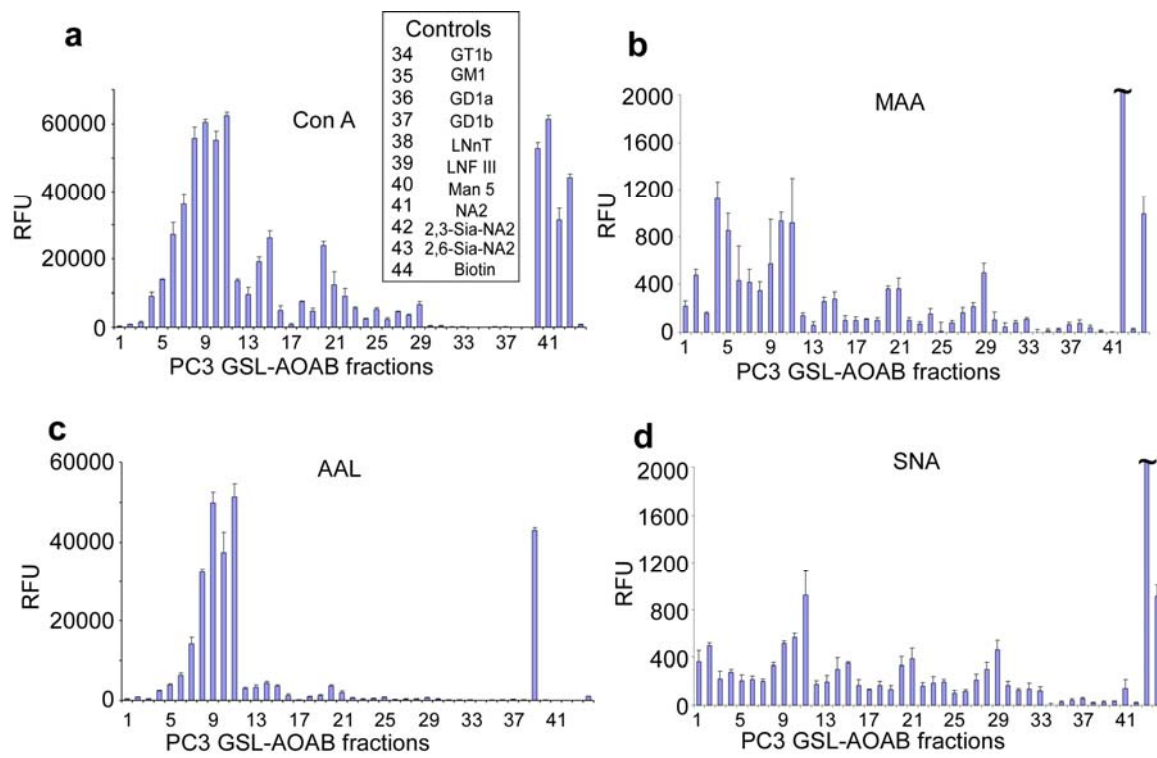


Supplementary Figure 4. The elucidation of the structure of fraction 12. Water loss can occur during MALDI analysis, however the loss of water can also occur prior to MALDI analysis as in a lactone or anhydrosugar formation. We offer multiple lines of evidence to support GD1b-lactone as the structure of fraction 12. These lines of evidence include: 1) C18 HPLC and MS analyses, which showed that upon storage this fraction separated into 2 major components with Peak 2 being the original component (the lactone) and Peak 1 being the hydrolyzed product from the lactone; 2) Neuraminidase treatment, showing resistance to neuraminidase as expected for a lactone; 3) Chemical treatment, since lactones are prone to amidation with amine while the corresponding disialyl GSLs and anhydrosugars are not. Based on these data, we are confident that the structure is a GD1b-lactone conjugate. **(a)** The C18-HPLC profiles of fraction #12 after ~1 year at -20°C storage (with several freeze-thaw cycles), Peak 1 (20.01 min) and Peak 2 (20.44 min) are annotated. The two peaks were isolated from HPLC and analyzed by mass spectrometry; **(b)** The MALDI-TOF spectra of Peak 1 (top panel), Peak 2 (middle panel), and the

MALDI-TOF/TOF spectrum of Peak 2 (bottom panel). Peak 1 showed a dominant molecular ion at m/z 1905 [M+H]⁺, matching (Hex₃HexNAc₁Neu5Ac₂) without loss of water. It is reasonable to conclude that peak 1 is formed by hydrolysis of the proposed lactone structure (Peak 2), which is consistent with Peak 2's longer retention time (greater hydrophobicity). **(c)** The C18-HPLC profiles of three fractions before and after neuraminidase treatment; Both GD1a-AOAB (fraction 24) and GD1b-AOAB (Peak 1 in fraction 12) were digested to GM1-AOAB (fraction 9) but the GD1b-lactone-AOAB (Peak 2 in fraction 12) is resistant to neuraminidase; **(d)** Ethylenediamine treatment of fraction 9 (GM1-AOAB) as a control and fraction 12. A new peak X is generated from GD1b-lactone-AOAB while GM1-AOAB and GD1b-AOAB are not affected. **(e)** The reaction scheme of GD1b-lactone-AOAB with ethylenediamine. The new peak X is isolated from HPLC and characterized by MALDI-TOF (top panel) and MALDI-TOF/TOF (bottom panel), which confirmed the expected molecular weight and fragmentation pattern of the amide of GD1b-AOAB.



Supplementary Figure 5. Fluorescent AOAB derivatization of PC3 cells GSLs. **(a)** C18-HPLC profile of the GSL-AOAB derivatives from a glycolipid extract of PC3 cells; **(b)** The MS analysis of fraction 16 and its tentative structure. In negative mode (top panel), this fraction showed only a single peak at 1535.1 $[\text{M}-\text{H}]^-$, suggesting an absolute mass of 1536. Interestingly, in positive mode, this fraction showed dominant peaks at 1456.8 $[\text{M}+\text{H}]^+$ and 1478.8 $[\text{M}+\text{Na}]^+$ (middle panel), with no detection at expected 1537 $[\text{M}+\text{H}]^+$. The striking discrepancy of the MS spectra in positive and negative mode clearly suggested a labile moiety with a mass of 80. While both sulfate and phosphate can give an 80 mass shift, it is known that de-sulfation is common while glycan phosphates are quite stable to fragmentation during MALDI-TOF analysis. Furthermore, the HPLC profile shift upon mild acid hydrolysis and resistance to alkaline phosphatase strongly suggests that the glycan associated with fraction 16 is sulfated. The 1456.8 $[\text{M}+\text{H}]^+$ molecular ion matches well with the composition of Hex₄HexNAc₁ possessing a C16-N-acyl sphingosine moiety. MS/MS analysis of peak 1456.8 (bottom panel) gave a clear linear pattern of Hex-HexNAc-Hex-Hex-Hex, suggesting a globo-series GSL structure with a sulfated pentasaccharide glycan.



Supplementary Figure 6. The lectin binding to PC3 cell glycosphingolipids microarray. Thirty-three fractions of PC3 GSL-AOABs were separated by C18-HPLC and printed; 11 GSL-AOAB or GAEAB structures were printed on the same microarray as controls. The concentration of lectins (**a**) ConA; (**b**) MAA; (**c**) AAL and (**d**) SNA used is $10 \mu\text{g ml}^{-1}$.

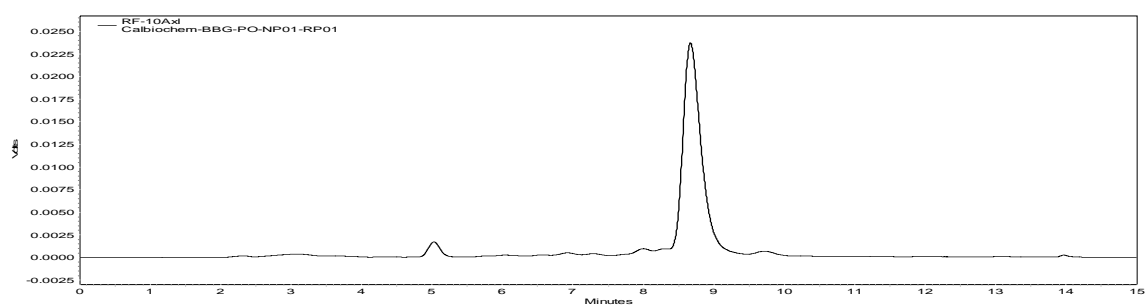
Supplementary Table 1. HPLC and Mass spectrometry characterization of BBG 2-dimensional fractions.

(a) All 40 fractions were characterized by MALDI-TOF/TOF and the MS and MS/MS spectra are included below. The major peaks and most probable glycan compositions are summarized in the following table. These fractions represent a tagged library of bovine brain gangliosides and were printed as described in the main text. The C18-HPLC profiles of the final re-purification are also attached below the table. All of the fractions (#1-40) are denoted on the profiles. For this re-purification, a linear gradient from 60% acetonitrile in 0.1% TFA to 90% acetonitrile in 0.1% TFA in 10 minutes was used.

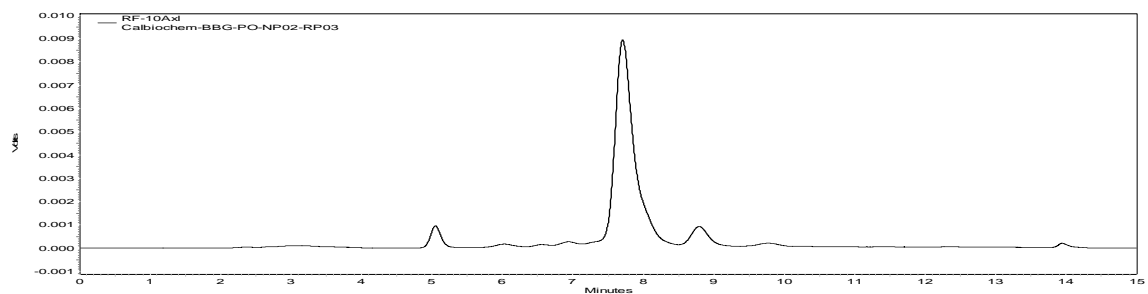
BBG-AOAB 2D fractions	NP fraction # and # retention time (min)	RP fraction # and retention time (min)	RP-HPLC repurify	Observed Mass (RP)	Observed Mass (RN)	Glycan Composition
F-01	NP01-28.34min	RP01-22.85		1248.766	1246.852	Hex2Neu5Ac1
F-02	NP02-29.09min	RP03-21.60		1344.701, 1025.492	1455.824	Hex3HexNAc1
F-03	NP03-30.35min	RP02-21.51		1613.943, 1823.134	1612.033	Hex3HexNAc1Neu5Ac1
F-04	NP03-30.35min	RP03-22.19		1451.87	1449.924	Hex2HexNAc1Neu5Ac1
F-05	NP03-30.35min	RP04-22.52		1521.884	1519.986, 1538.003	Hex2Neu5Ac2-H2O
F-06	NP04-31.16min	RP03-23.88		1583.895, 1793.1	1581.978	Hex3HexNAc1Neu5Ac1
F-07	NP05-31.72min	RP01-21.58		1887.175	1885.145	Hex3HexNAc1Neu5Ac2-H2O
F-08	NP06-32.70min	RP03-21.05		1376.663	1336.779	Hex3HexNAc1Neu5Ac1
F-09	NP06-32.70min	RP04-22.04		1614.03	1612.152	Hex3HexNAc1Neu5Ac1
F-10	NP07-34.76min	RP01-20.27		1390.71	1366.797, 1609.876	Hex3HexNAc1Neu5Ac2
F-11	NP07-34.76min	RP02-20.72		1887.057	1886.029, 1904.064	Hex3HexNAc1Neu5Ac2-H2O
F-12	NP07-34.76min	RP03-20.99		1887.052	1886.042	Hex3HexNAc1Neu5Ac2-H2O
F-13	NP07-34.76min	RP04-21.57		1613.941	1612.072	Hex3HexNAc1Neu5Ac1
F-14	NP07-34.76min	RP05-22.08		1614.195	1612.127	Hex3HexNAc1Neu5Ac1
F-15	NP08-36.52min	RP01-19.56		1685.771	1639.9	Hex3HexNAc1Neu5Ac2
F-16	NP08-36.52min	RP03-20.74		1817.455	1815.44	Hex3HexNAc2Neu5Ac1
F-17	NP08-36.52min	RP06-23.63		1509.816	1485.867	Hex3HexNAc1Neu5Ac1
F-18	NP09-38.12min	RP03-20.48		1593.719	1570.049	Hex3HexNAc2Neu5Ac1
F-19	NP09-38.12min	RP04-21.04		2020.099	2018.157	Hex3HexNAc3Neu5Ac1
F-20	NP09-38.12min	RP06-22.65		1522.028	1520.033	Hex2Neu5Ac2-H2O
F-21	NP09-38.12min	RP07-23.60		1782.876, 1875.06	1740.892	Hex3HexNAc1Neu5Ac2
F-22	NP10-38.49min	RP08-23.51		1874.979	1895.103	Hex3HexNAc1Neu5Ac2
F-23	NP11-40.46min	RP02-20.30		2108.3	2128.412	Hex3HexNAc2Neu5Ac2
F-24	NP11-40.46min	RP03-21.78		1905.15	1885.225	Hex3HexNAc1Neu5Ac2

F-25	NP11-40.46min	RP04-23.50		1629.864	2208.283	Hex3HexNAc1Neu5Ac3-H2O
F-26	NP12-42.3min	RP01-20.23		1681.946, 1756.127	1640.054	Hex3HexNAc1Neu5Ac2
F-27	NP12-42.3min	RP02-20.70	a	2178.554, 2196.576	2176.605	Hex3HexNAc1Neu5Ac3-H2O
F-28	NP12-42.3min	RP02-20.70	b	2178.255	2176.523	Hex3HexNAc1Neu5Ac3-H2O
F-29	NP12-42.3min	RP02-20.70	c	1887.030, 2178.135	2094.3	Hex3HexNAc1Neu5Ac3-H2O
F-30	NP12-42.3min	RP03-21.60		1404.58	1380.755	Hex3HexNAc1Neu5Ac1
F-31	NP14-46.4min	RP06-23.52		1801.09	1758.933	Hex3HexNAc1Neu5Ac2
F-32	NP17-50.83min	RP01-20.37	a	2193.972, 2212.007	2210.433	Hex3HexNAc1Neu5Ac2Neu5Gc
						Hex3HexNAc1Neu5Ac2Neu5Gc-H2O
F-33	NP17-50.83min	RP01-20.37	b	2194.168	2214.479	
F-34	NP18-52.88min	RP02-19.91	a	2178.128	2194.29	Hex3HexNAc1Neu5Ac3-H2O
F-35	NP18-52.88min	RP02-19.91	b	2178.224	2176.365	Hex3HexNAc1Neu5Ac3-H2O
F-36	NP18-52.88min	RP03-20.43	a	2177.943	2198.369	Hex3HexNAc1Neu5Ac3-H2O
F-37	NP18-52.88min	RP03-20.43	b	2178.492	2198.499	Hex3HexNAc1Neu5Ac3-H2O
F-38	NP19-55.00min	RP01-20.20	a	2451.852	2467.703	Hex3HexNAc1Neu5Ac4-2H2O
F-39	NP19-55.00min	RP01-20.20	b	2178.612	2467.557	Hex3HexNAc1Neu5Ac4-2H2O
F-40	NP20-57~69min	RP01-21.36		1695.854	1654.123	Hex3HexNAc1Neu5Ac2

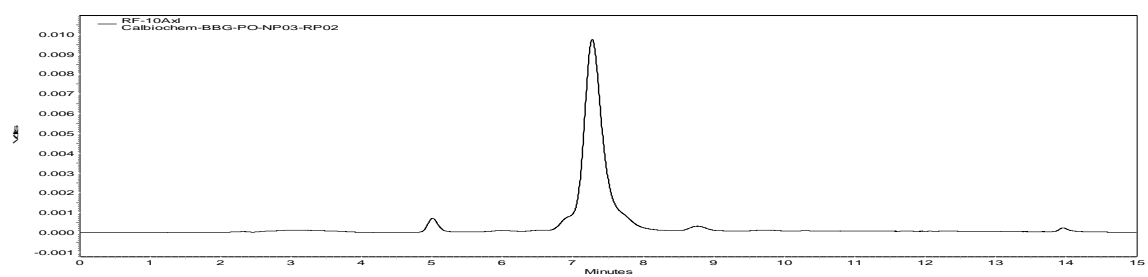
(b) Re-chromatography of all 40 HPLC fractions on C18 HPLC.
F-01



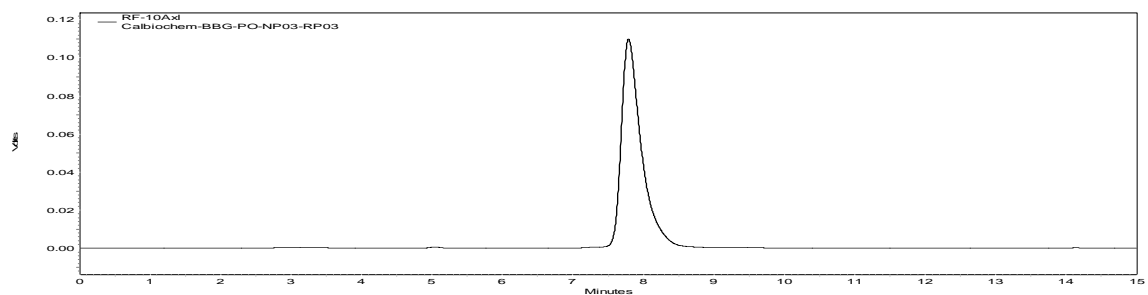
F-02



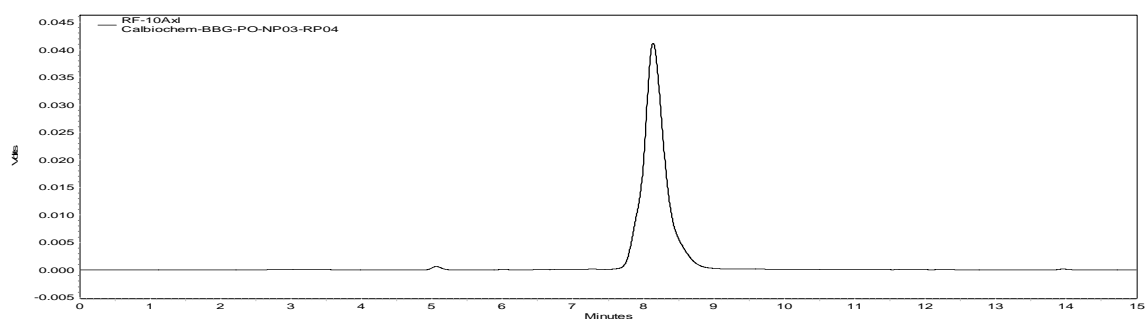
F-03



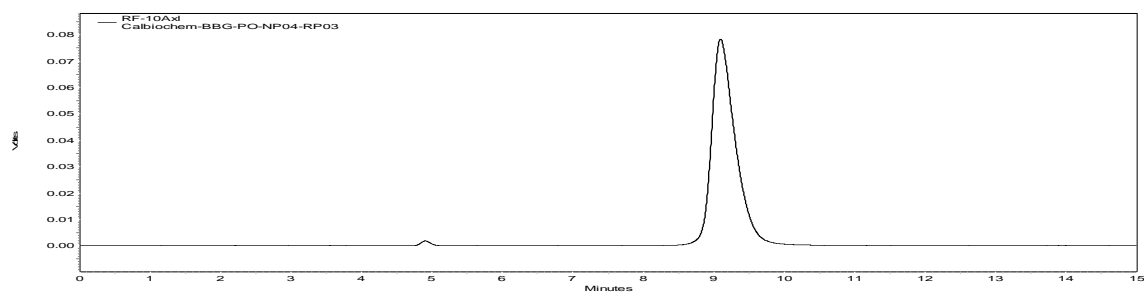
F-04



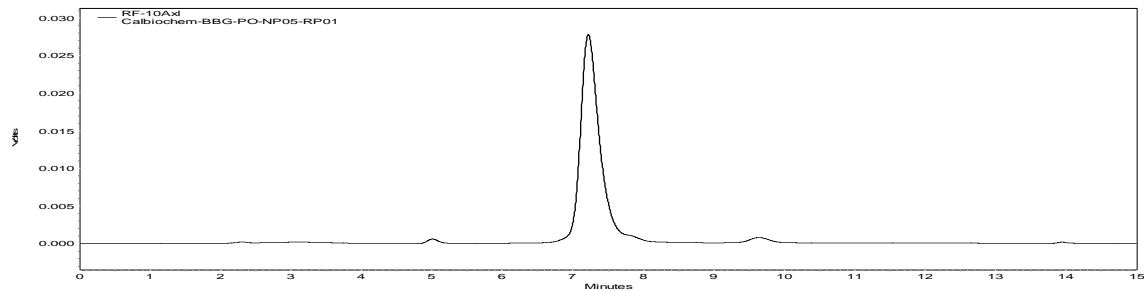
F-05



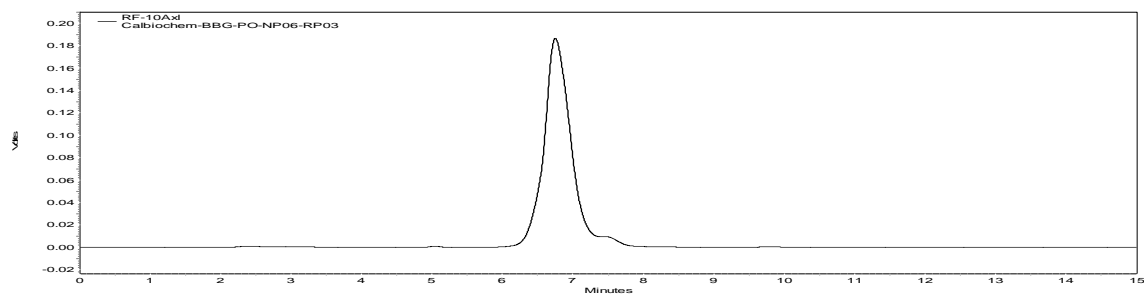
F-06



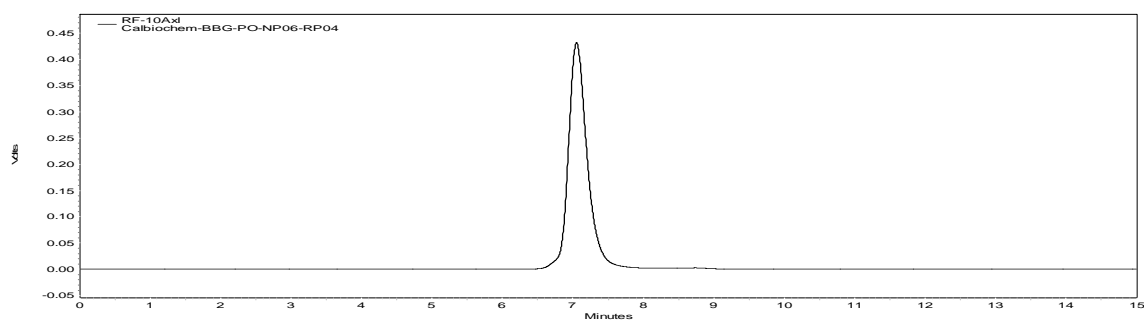
F-07



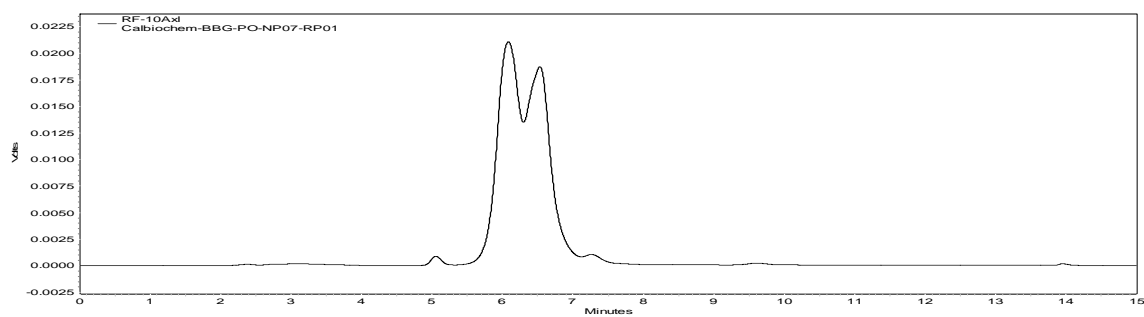
F-08



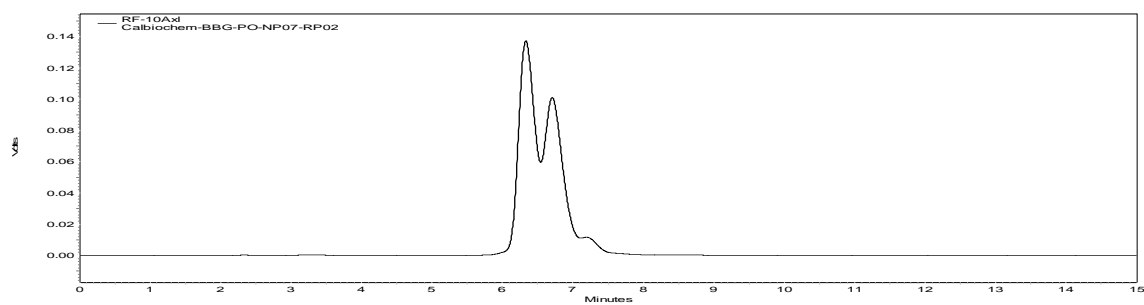
F-09



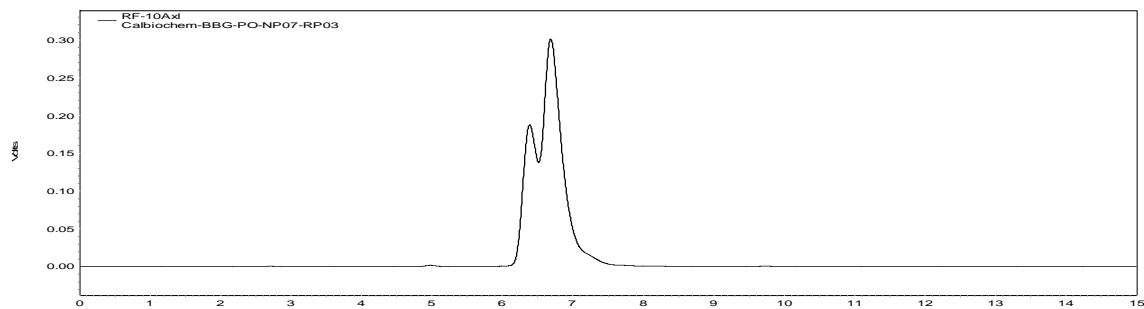
F-10



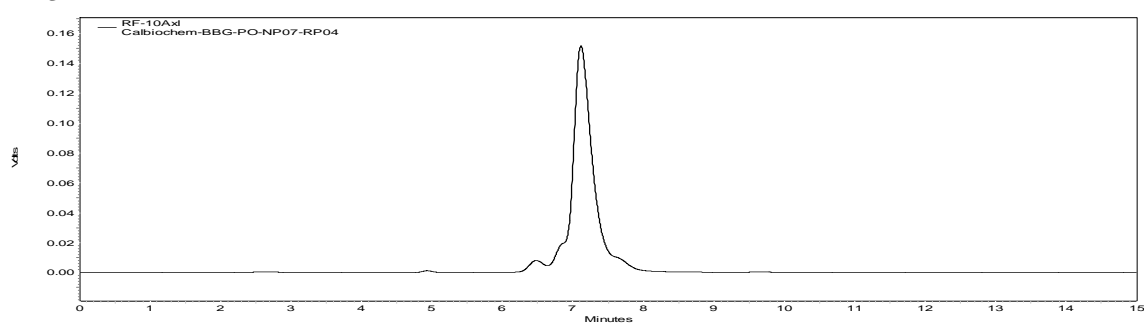
F-11



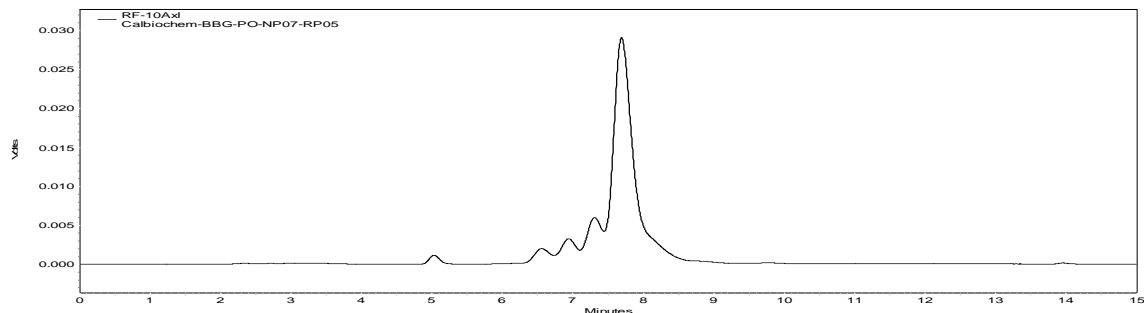
F-12



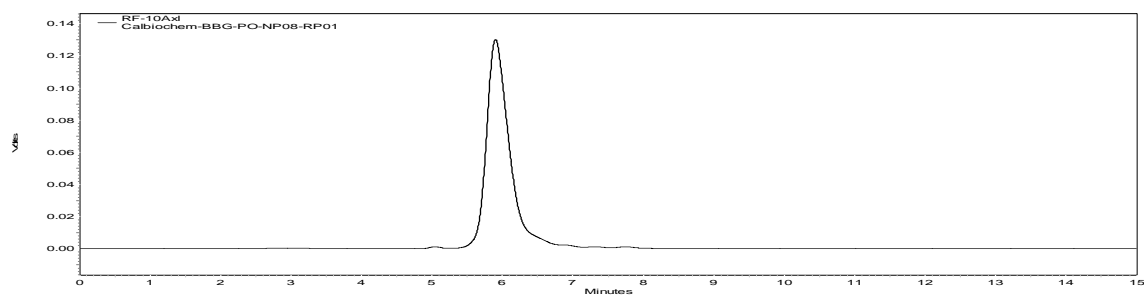
F-13



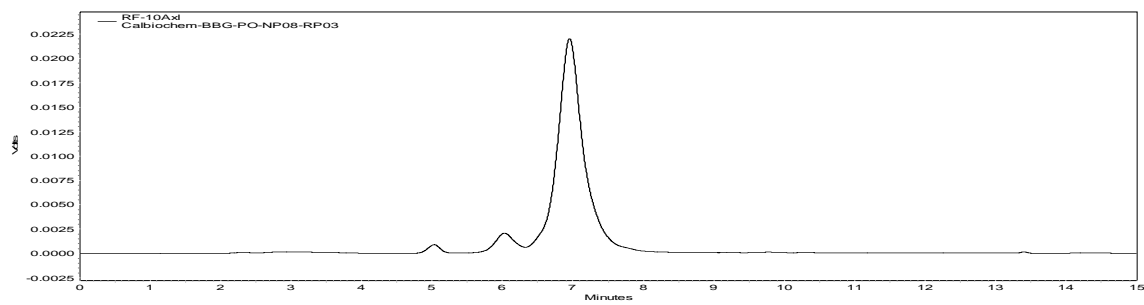
F-14



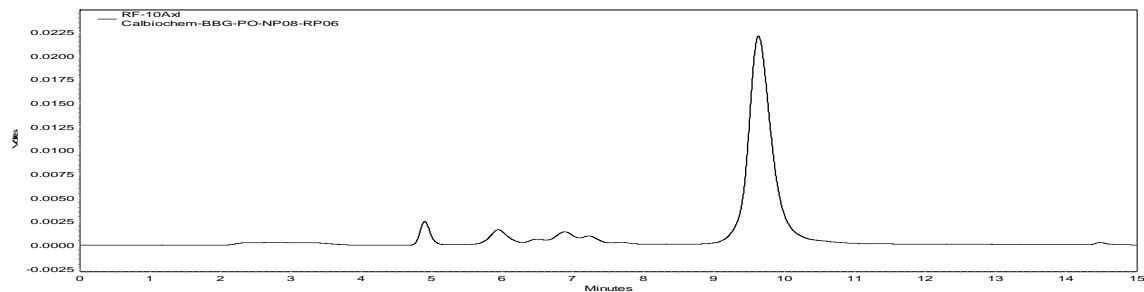
F-15



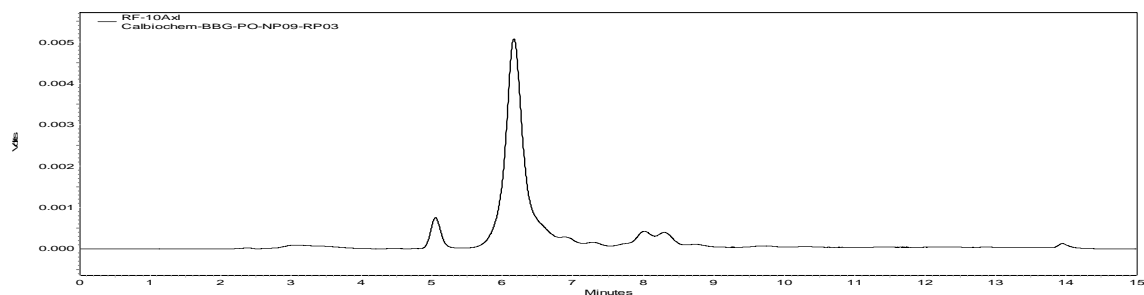
F-16



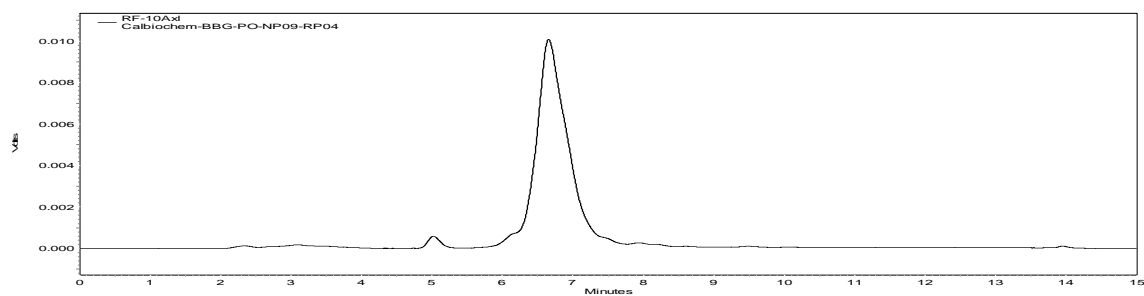
F-17



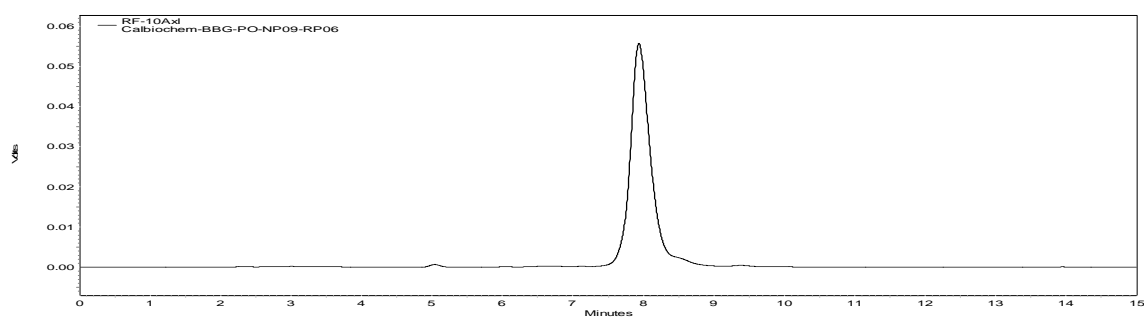
F-18



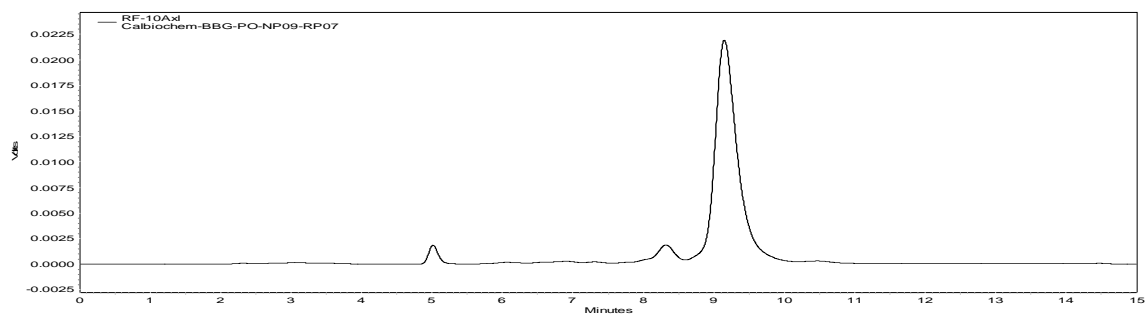
F-19



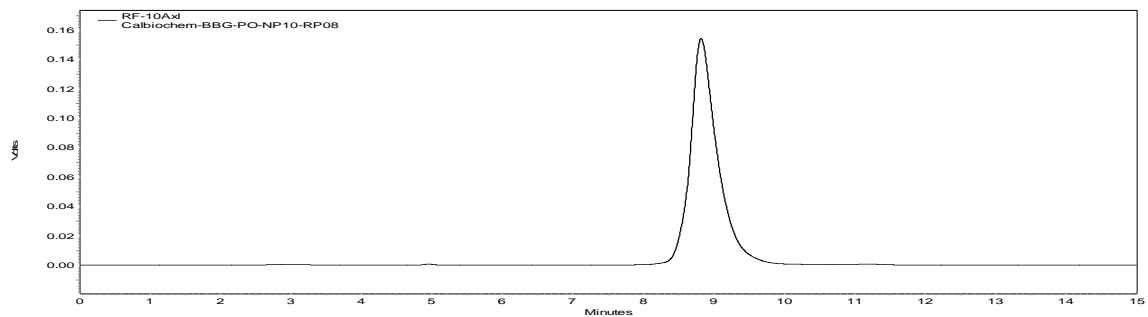
F-20



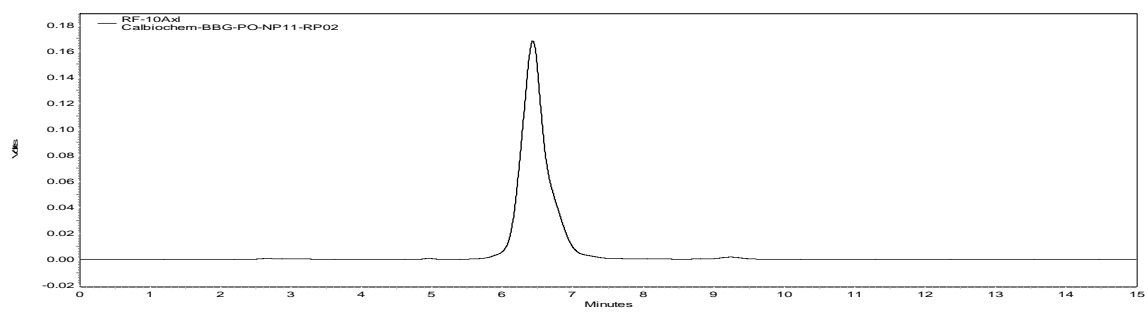
F-21



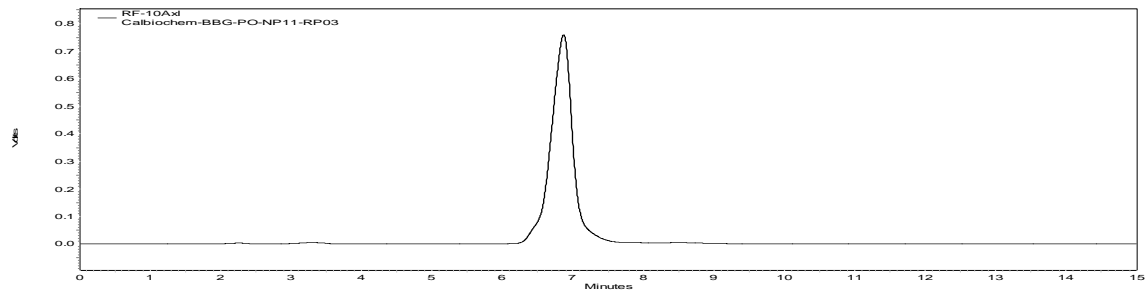
F-22



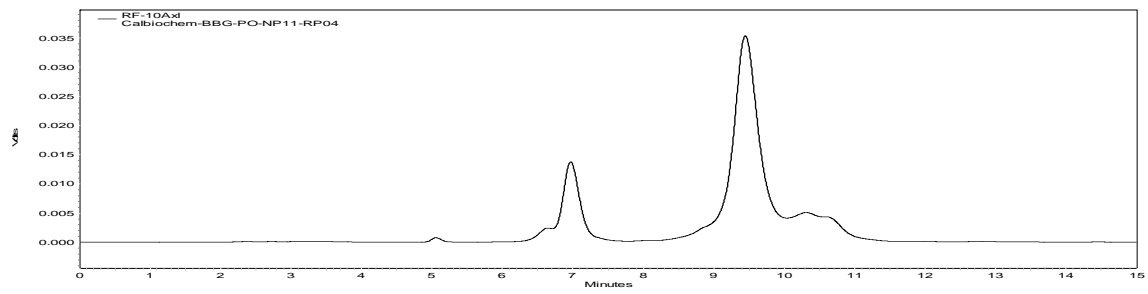
F-23



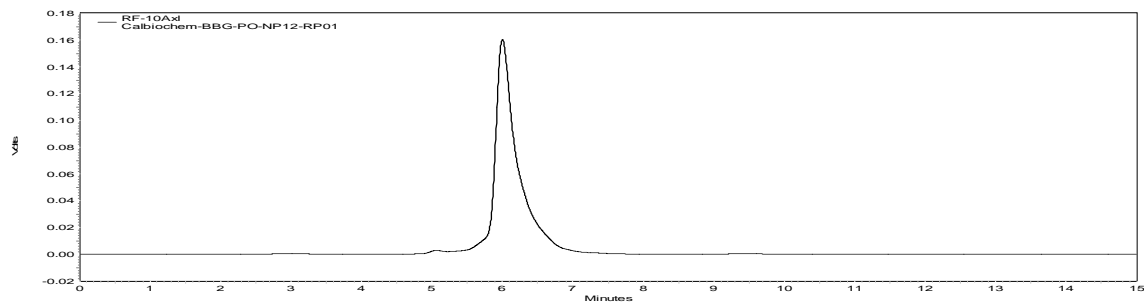
F-24



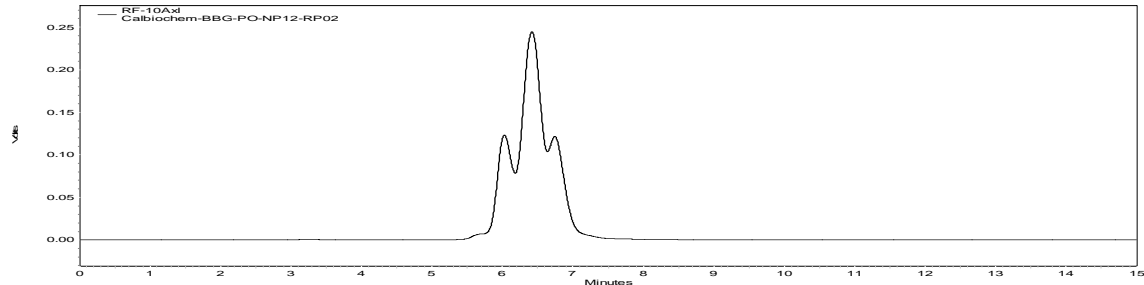
F-25



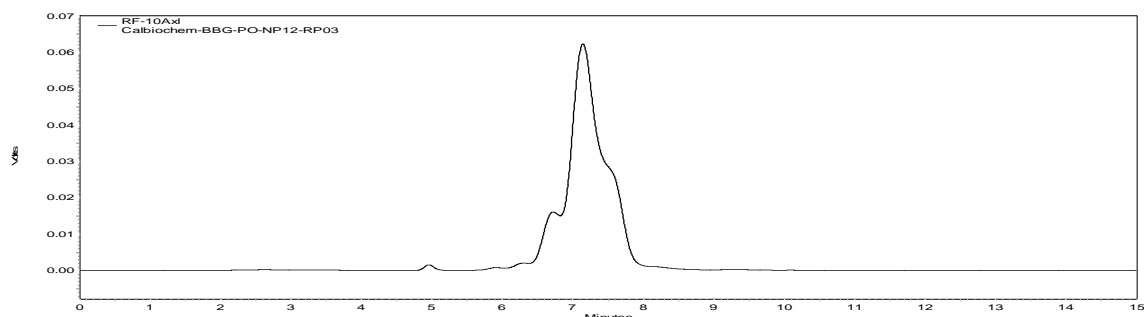
F-26



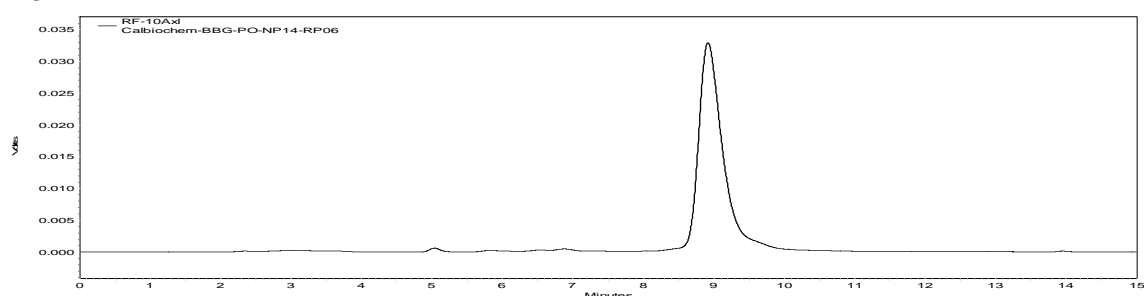
F-27, 28, 29 (left, middle and right peaks respectively)



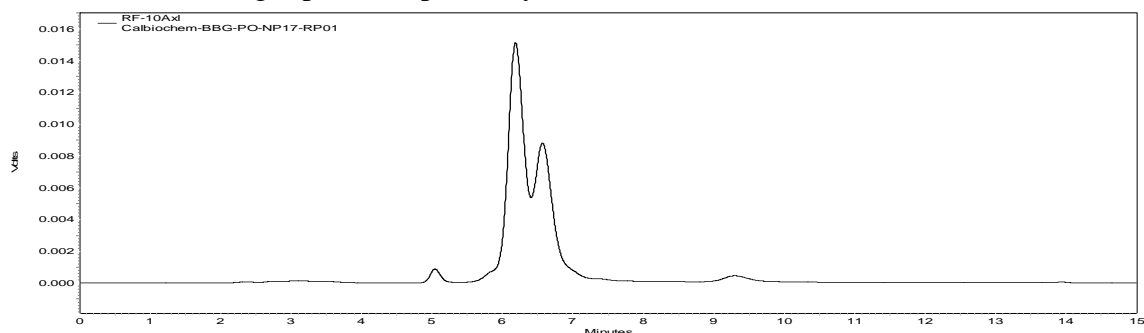
F-30



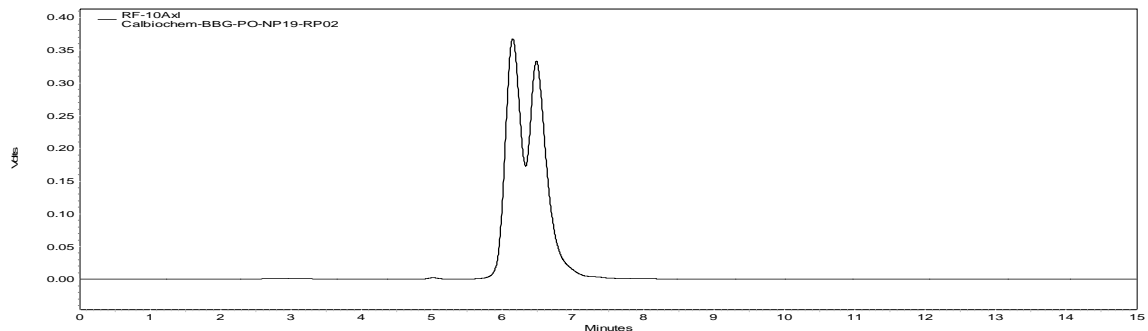
F-31



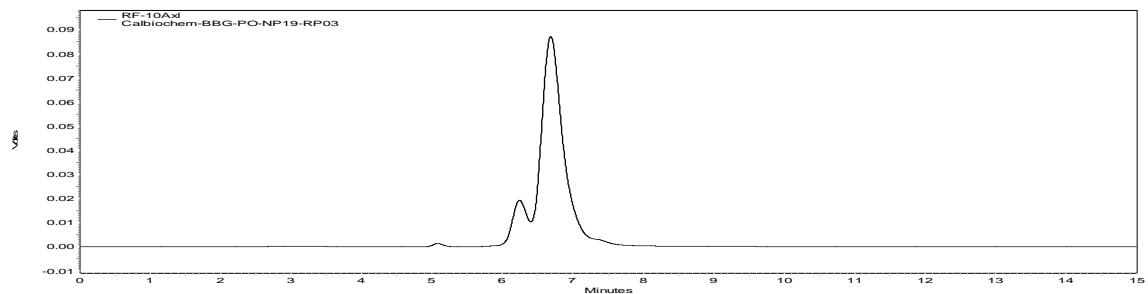
F-32, 33 (left and right peaks respectively)



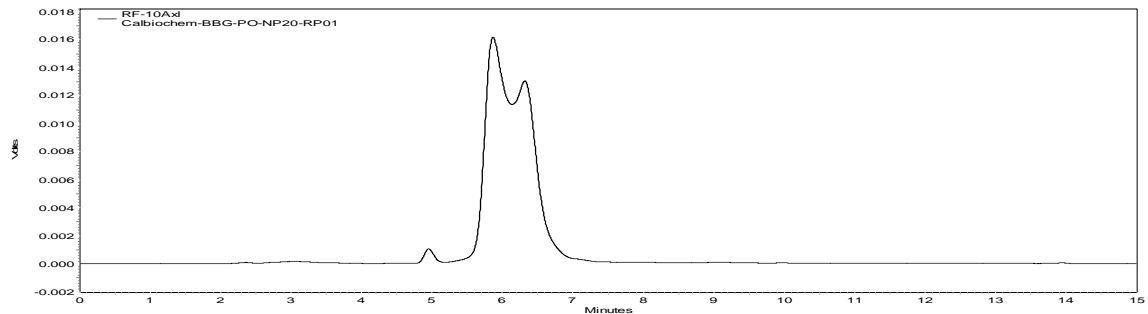
F-34, 35 (left and right peaks respectively)



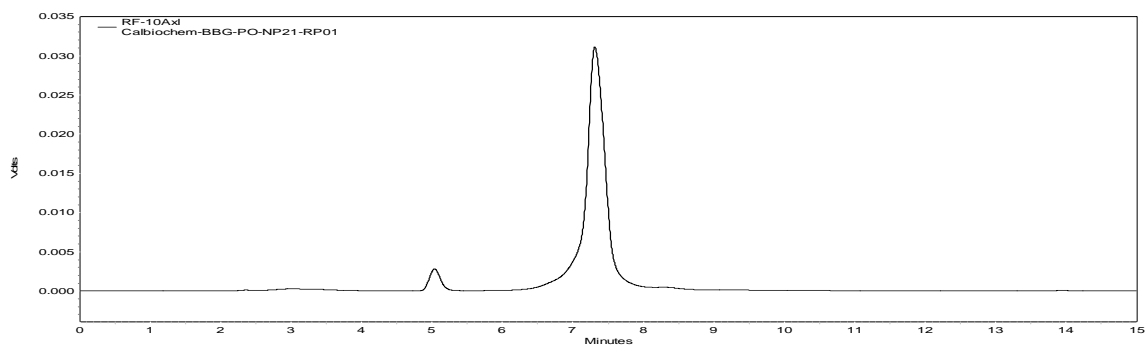
F-36, 37 (left and right peaks respectively)



F-38, 39 (left and right peaks respectively)

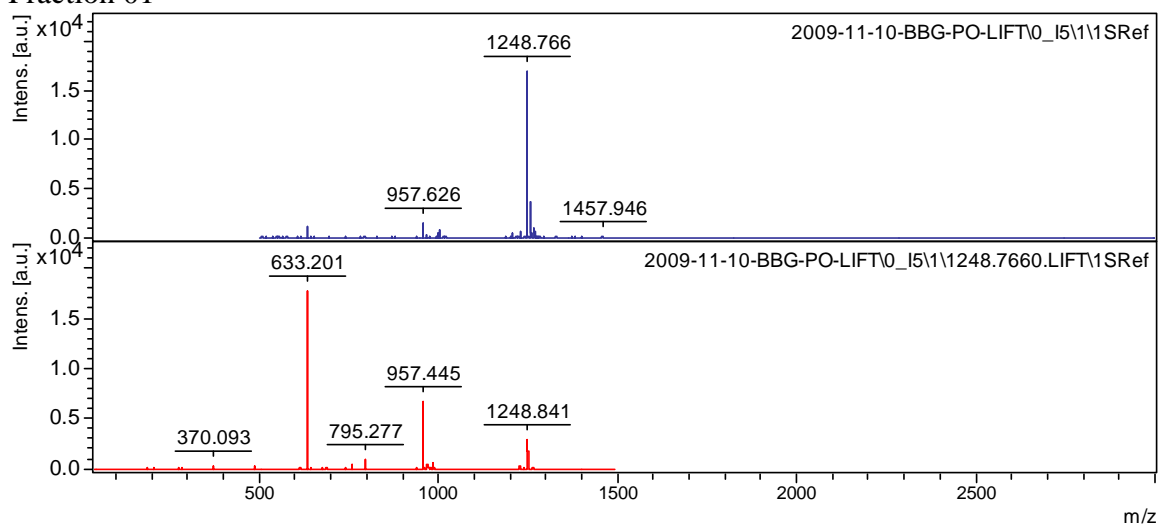


F-40

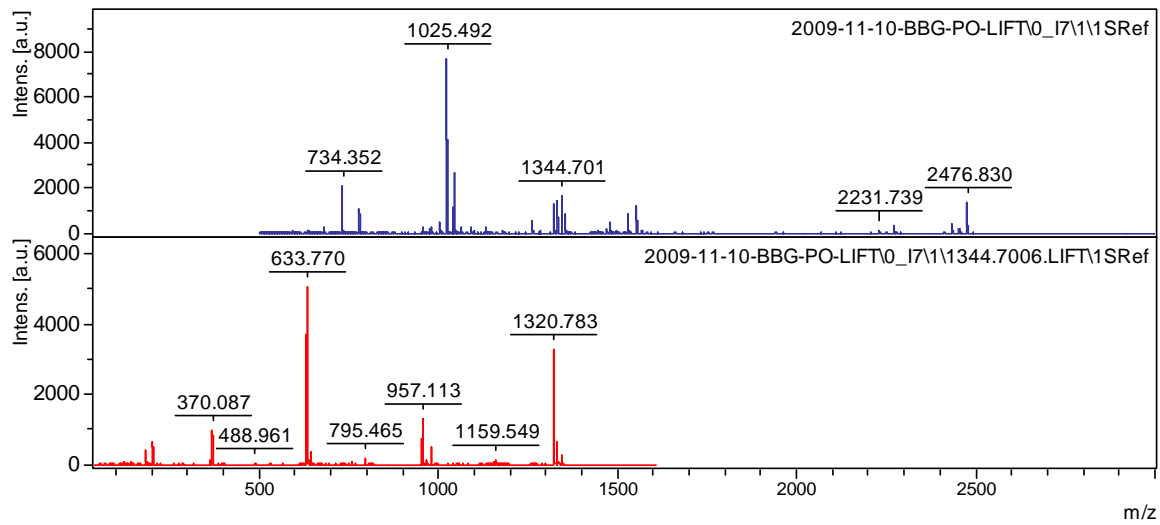


(c) MS and MS/MS spectra of the 40 fractions.

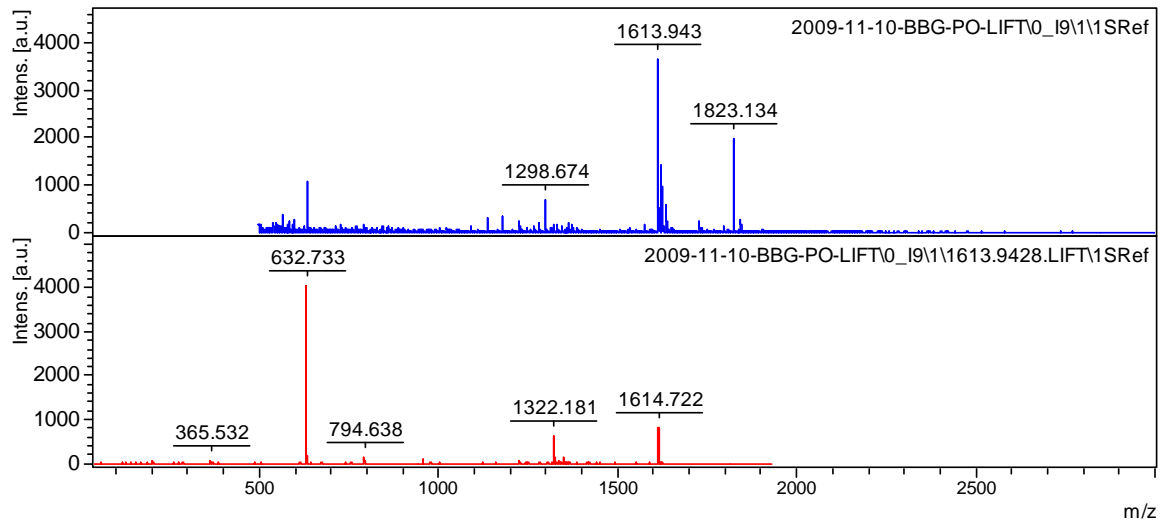
Fraction 01



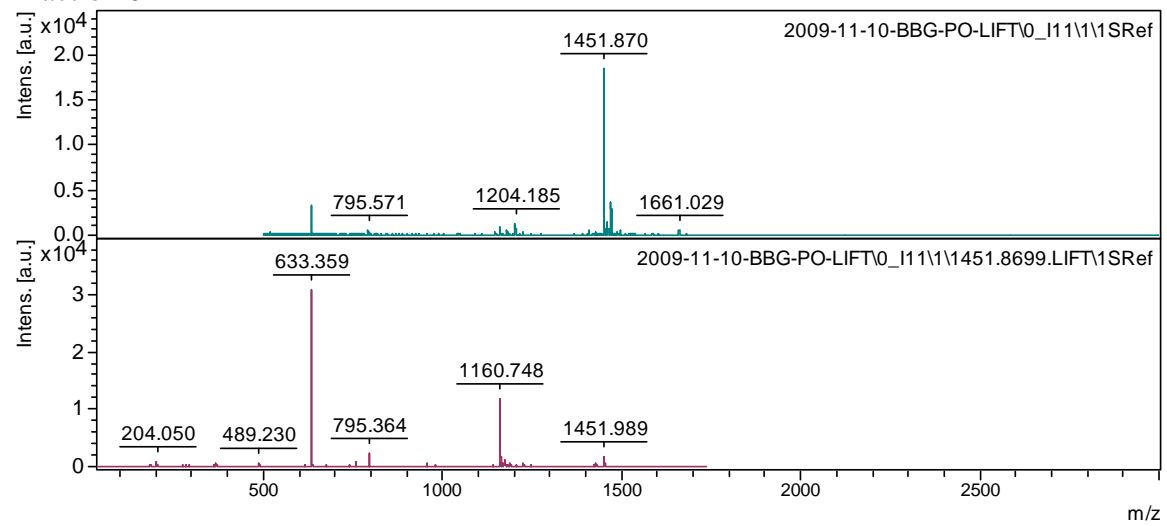
Fraction 02



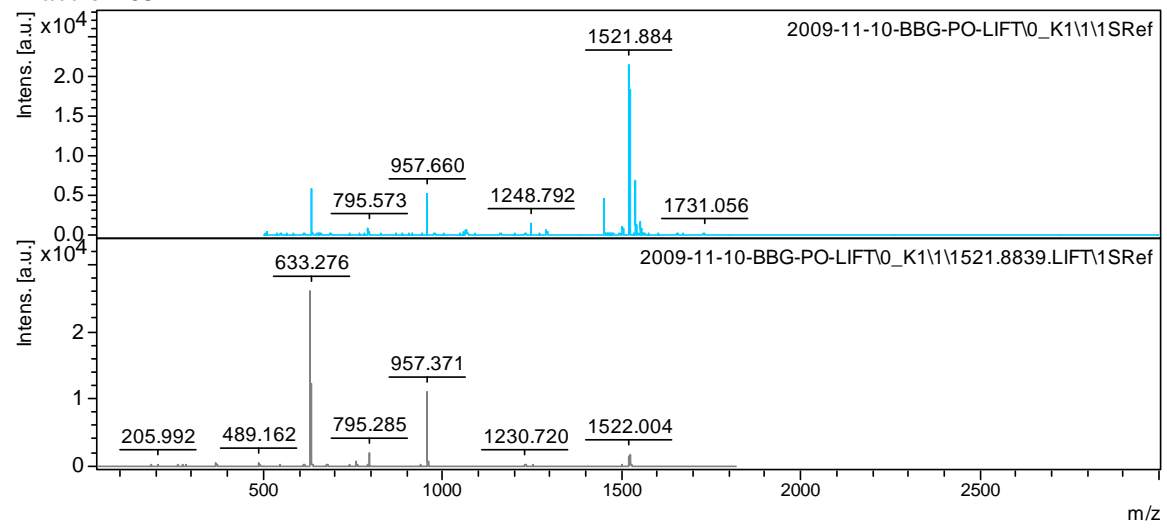
Fraction 03



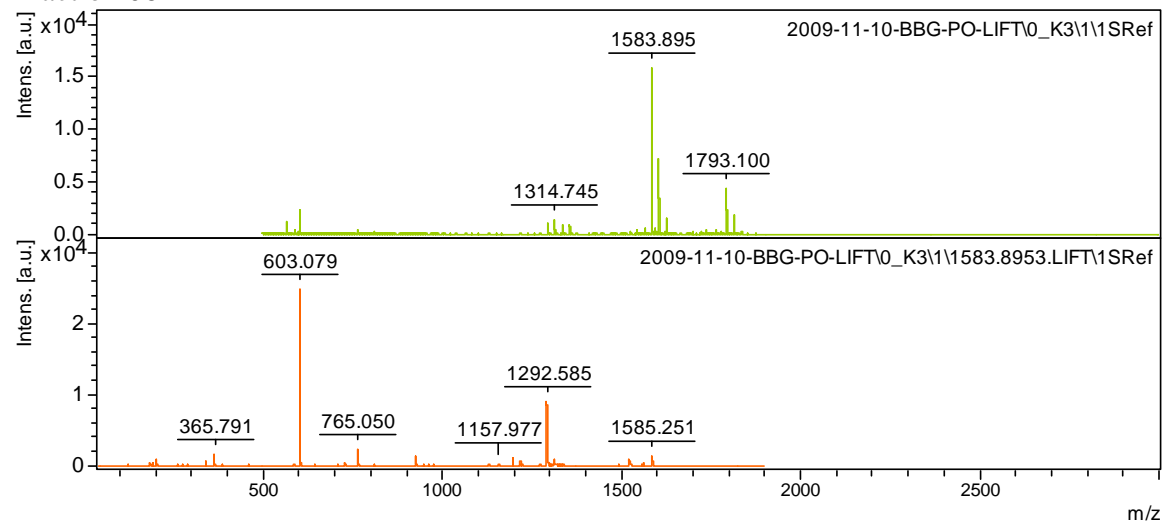
Fraction 04



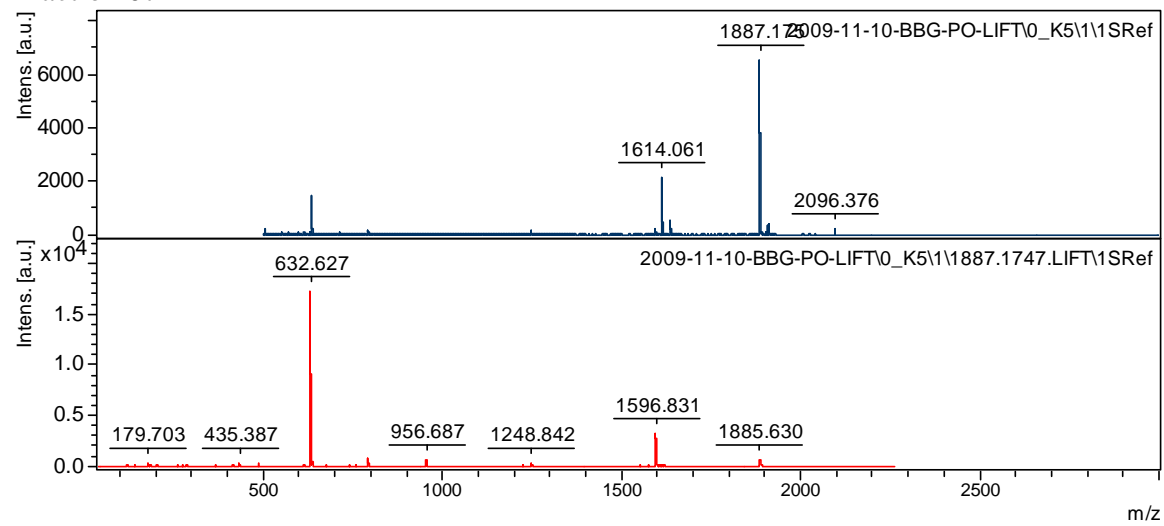
Fraction 05



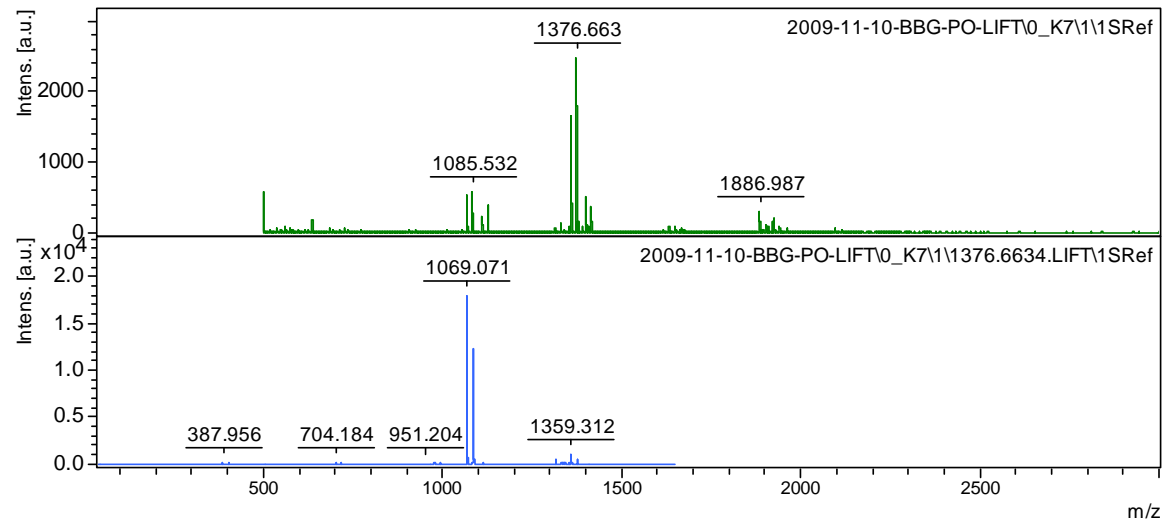
Fraction 06



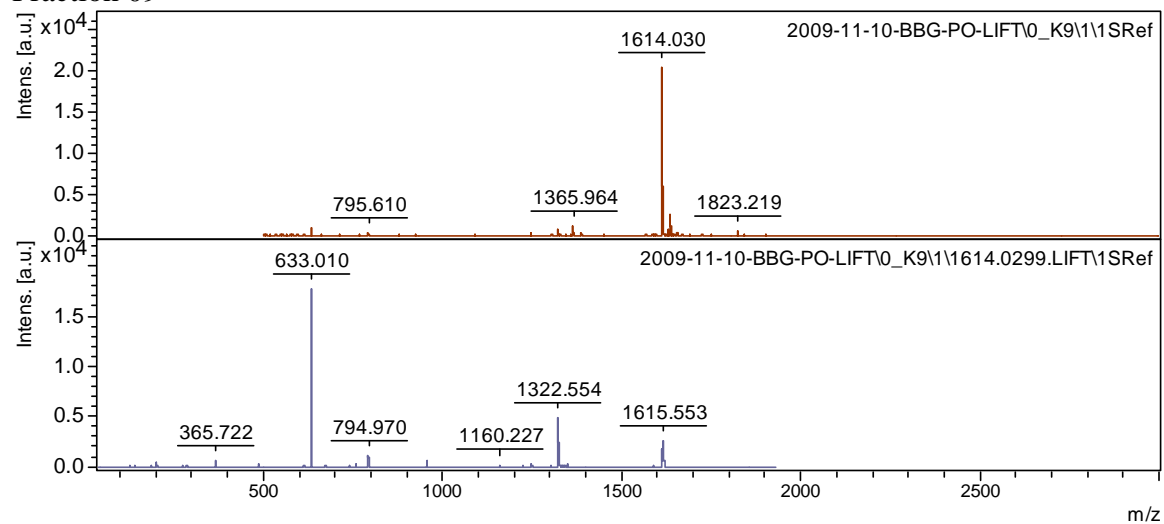
Fraction 07



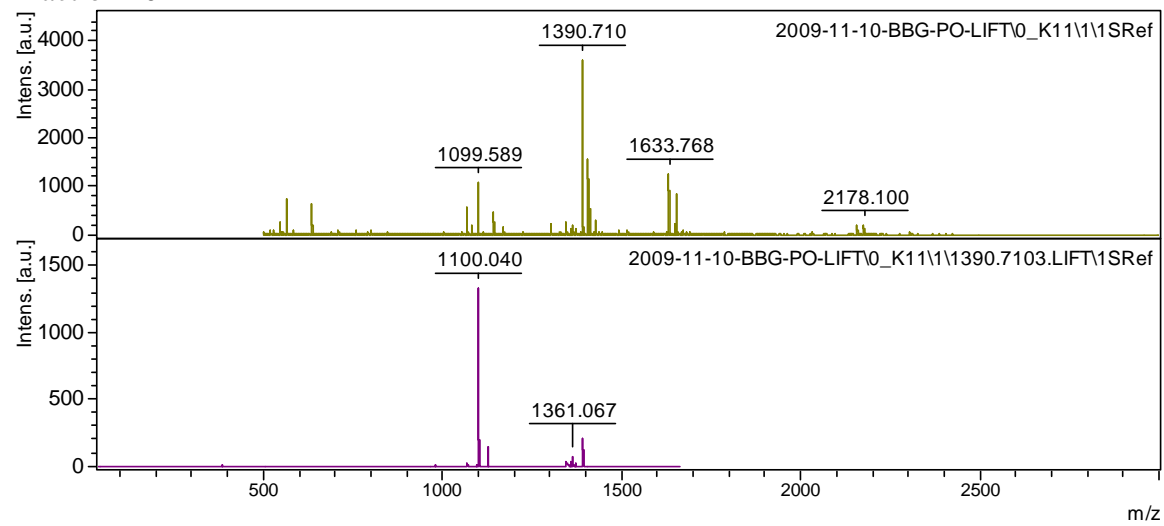
Fraction 08



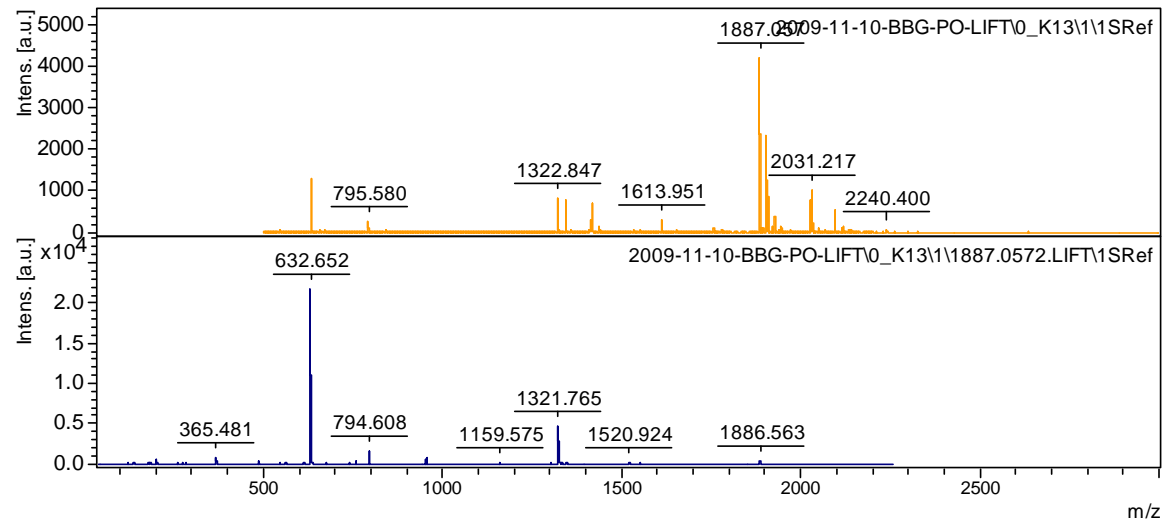
Fraction 09



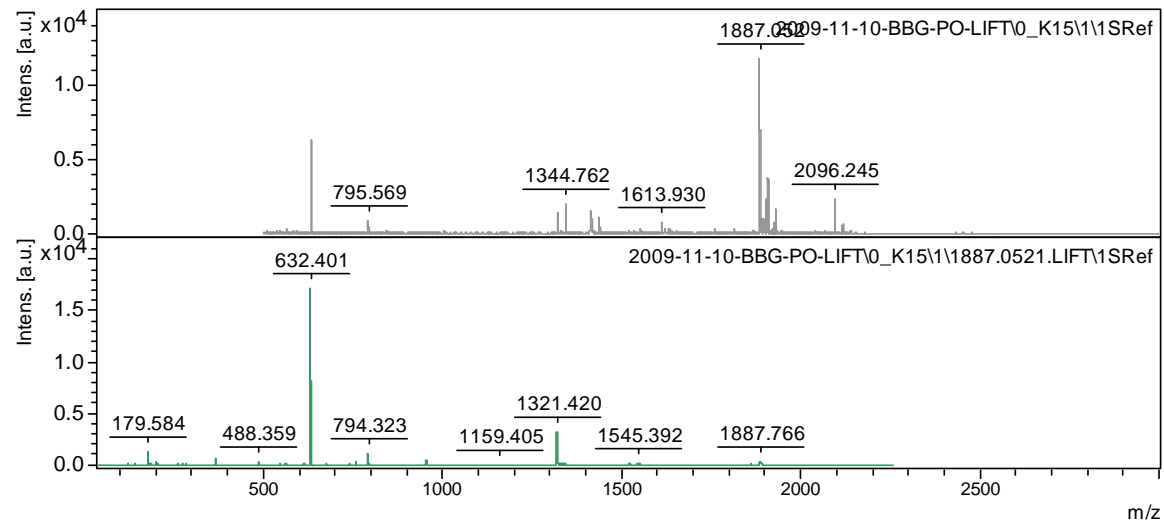
Fraction 10



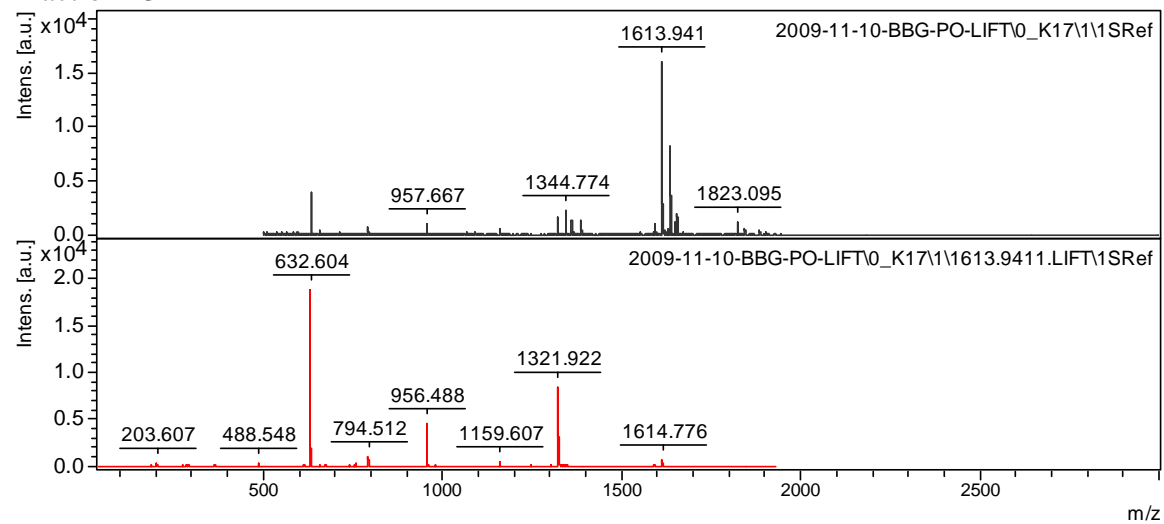
Fraction 11



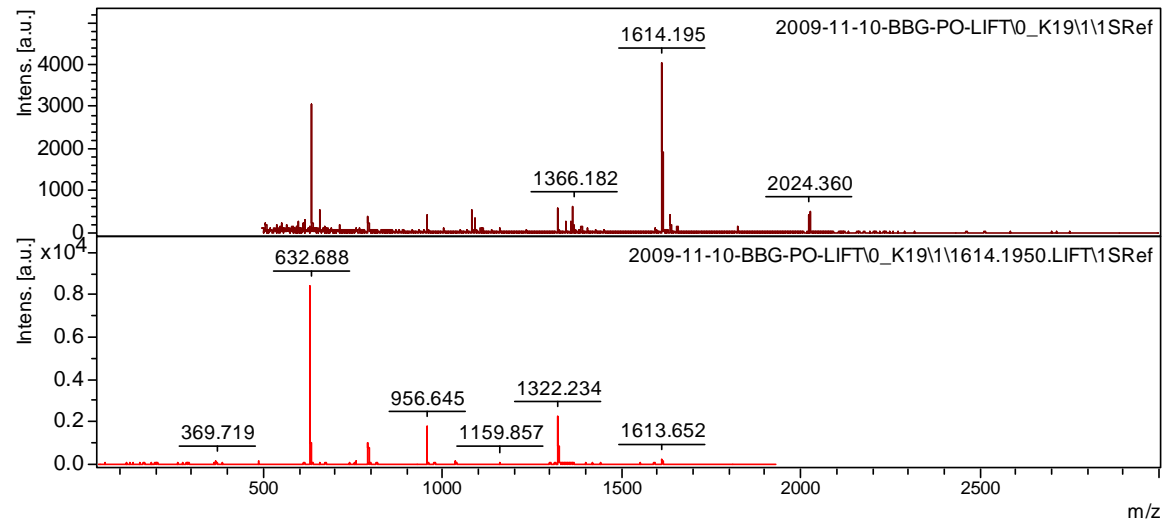
Fraction 12



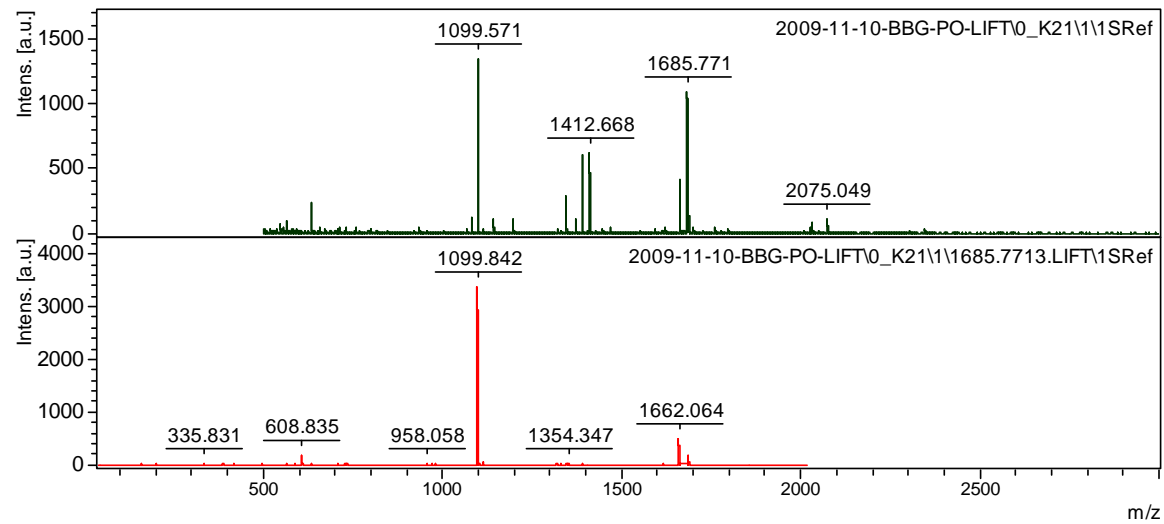
Fraction 13



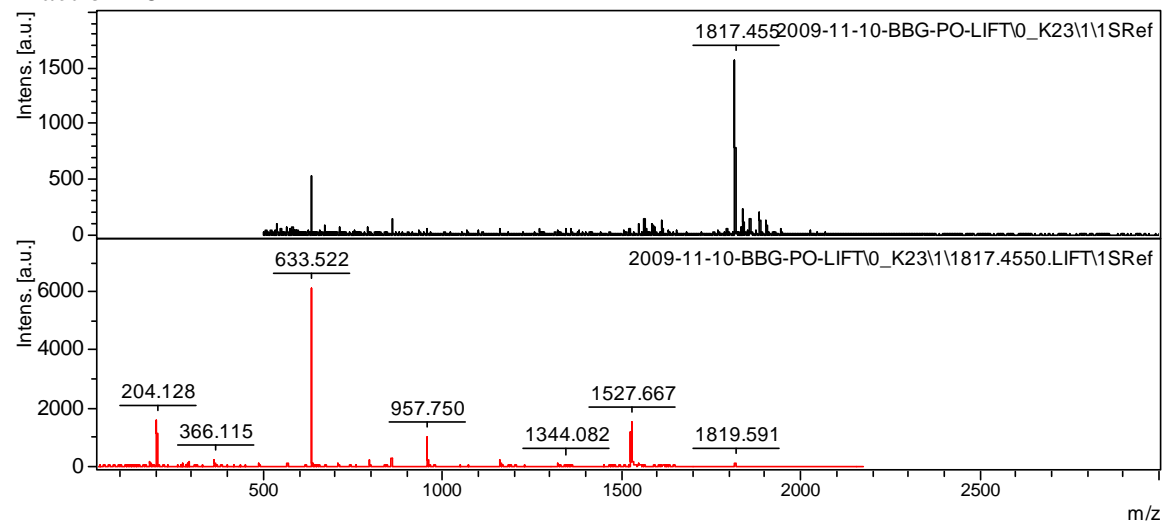
Fraction 14



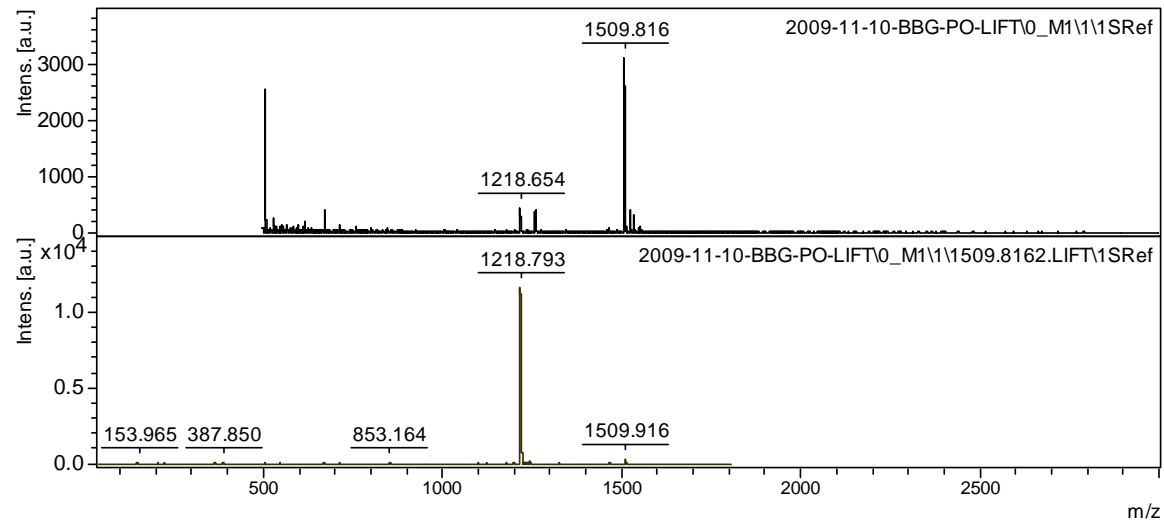
Fraction 15



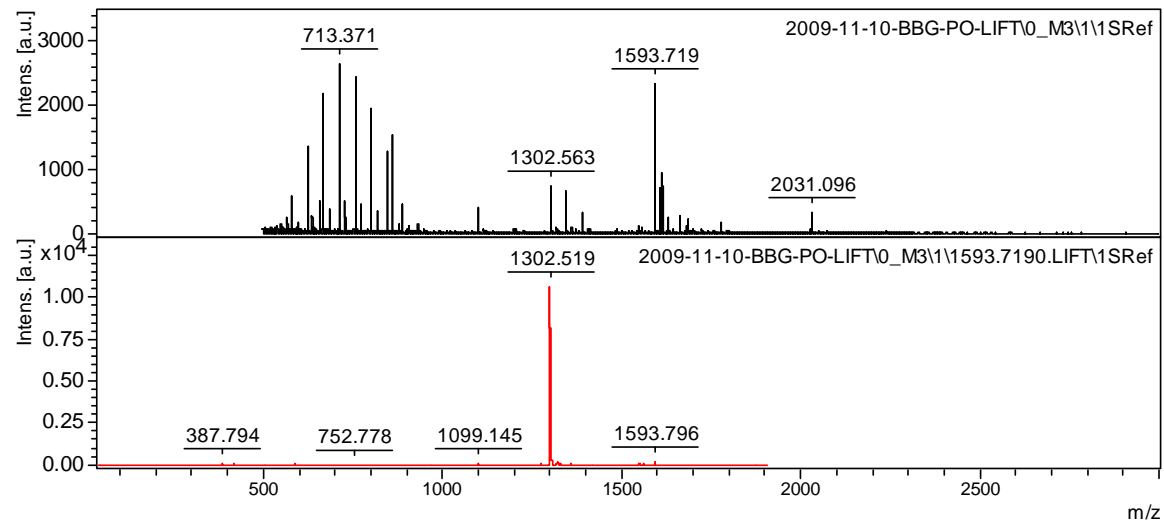
Fraction 16



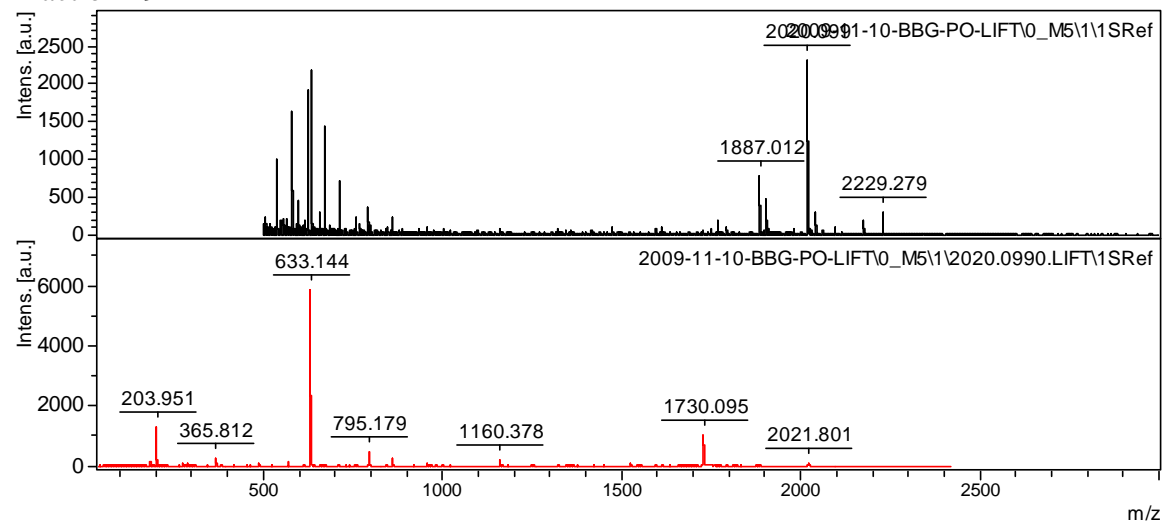
Fraction 17



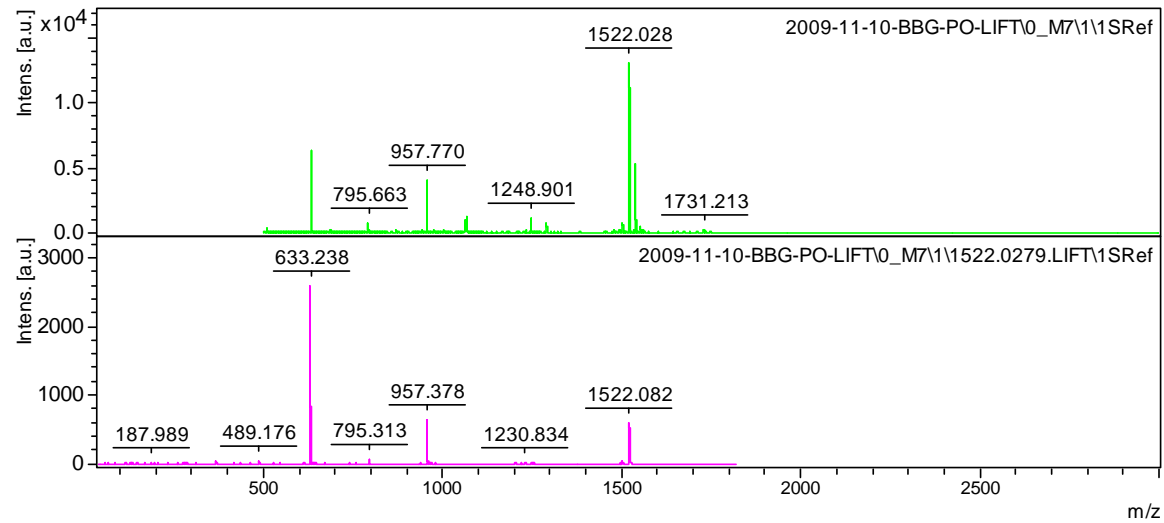
Fraction 18



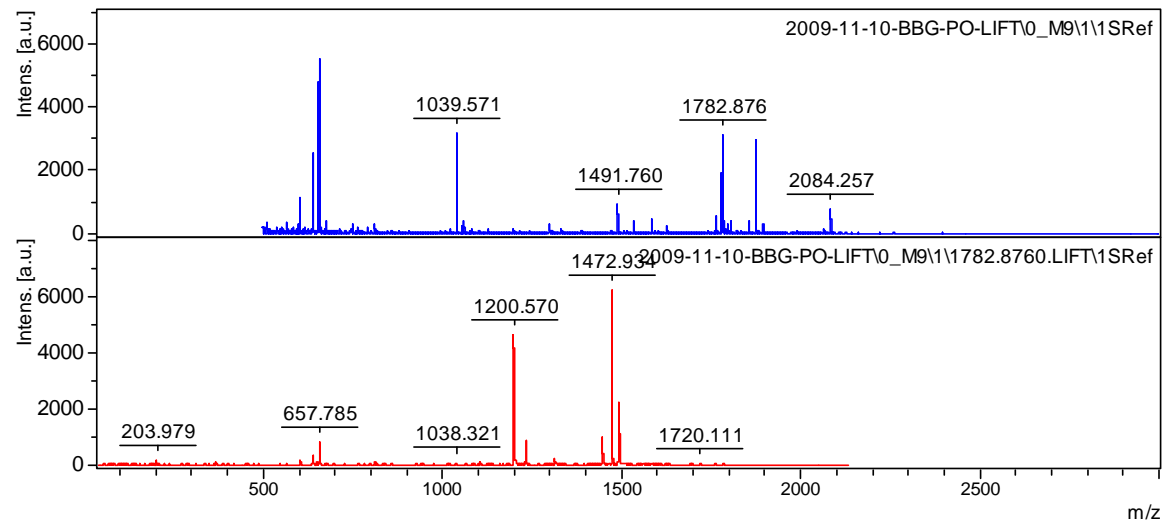
Fraction 19



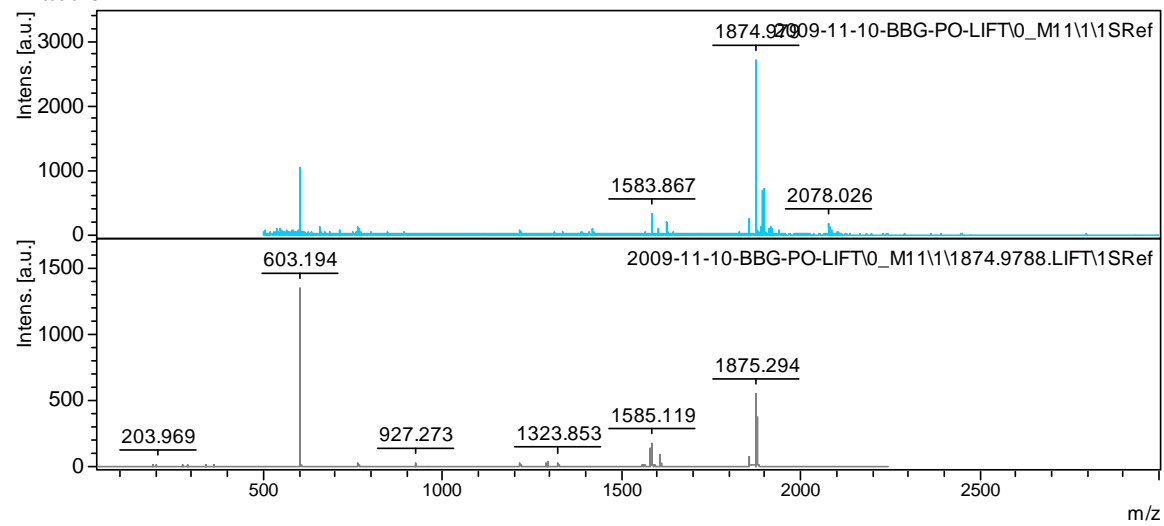
Fraction 20



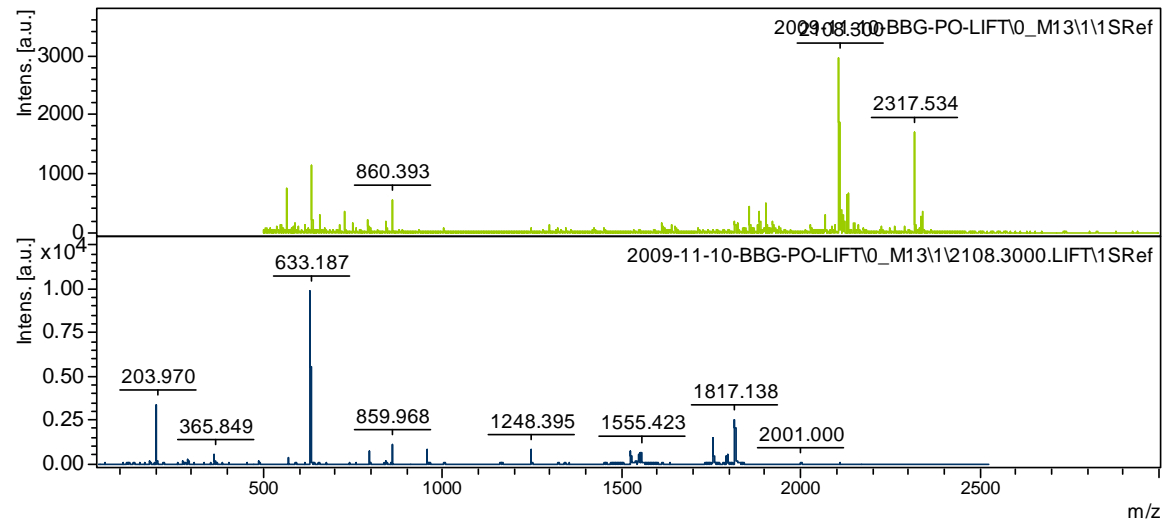
Fraction 21



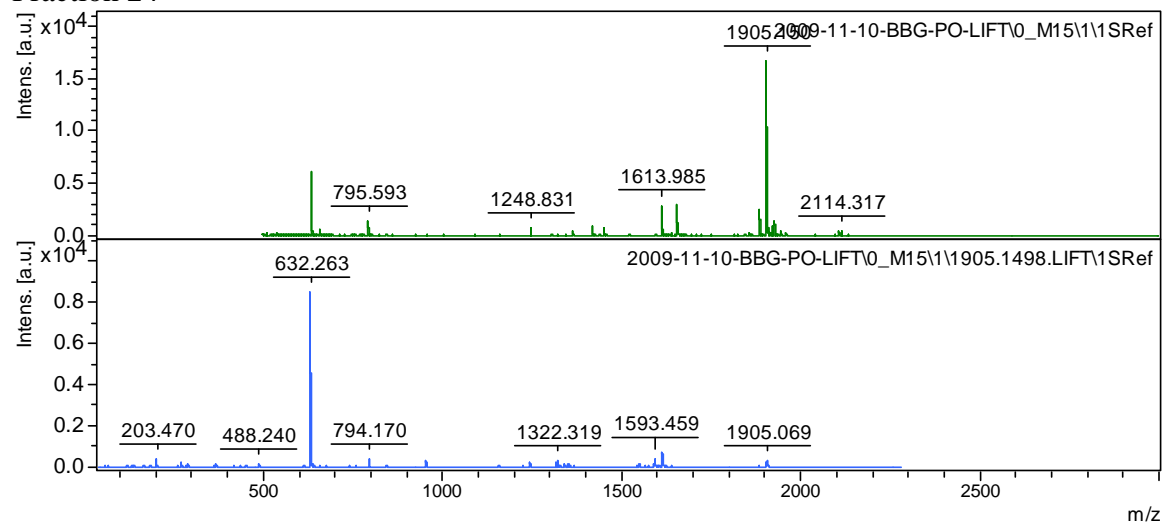
Fraction 22



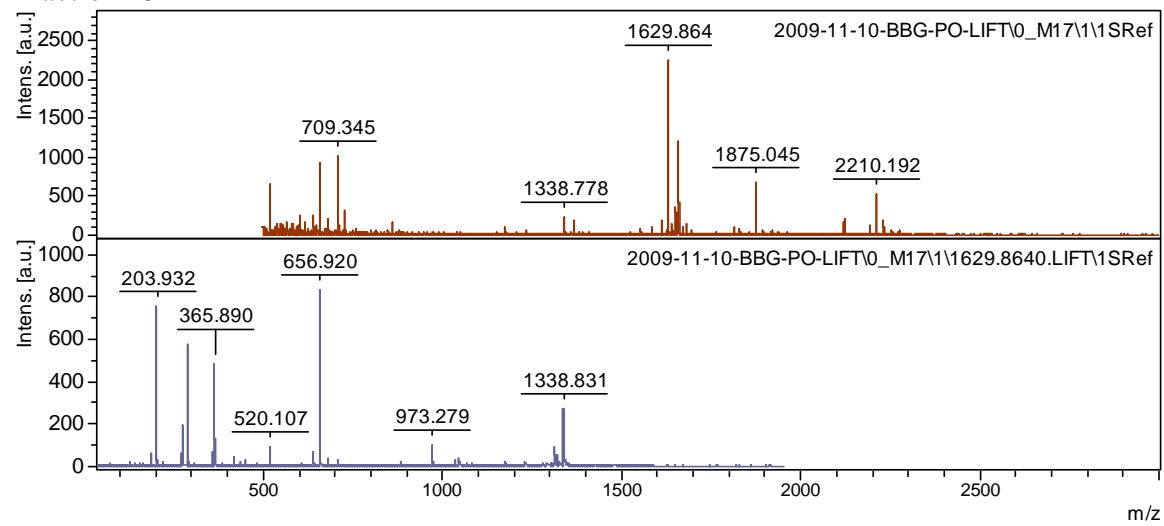
Fraction 23



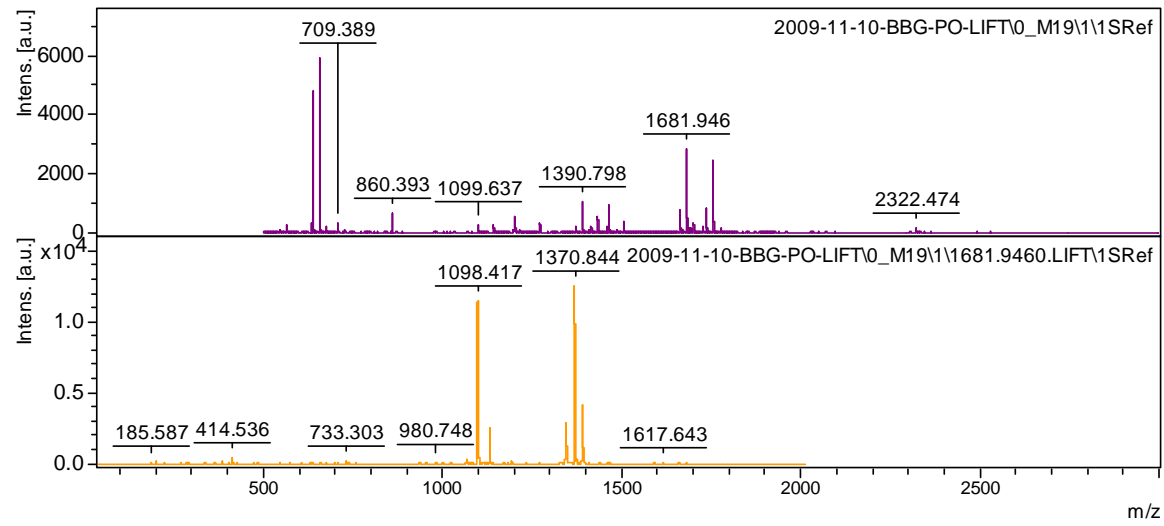
Fraction 24



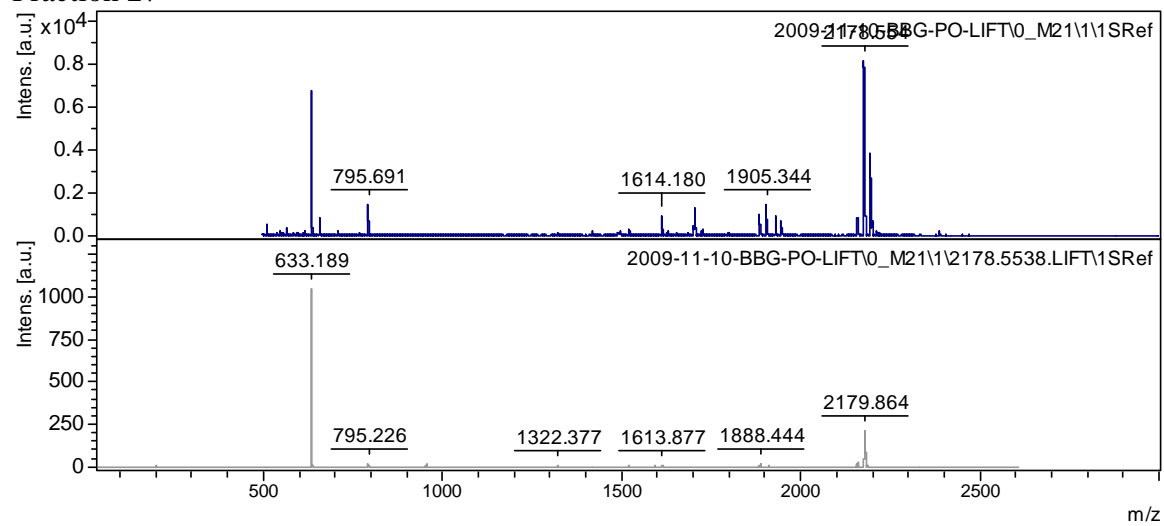
Fraction 25



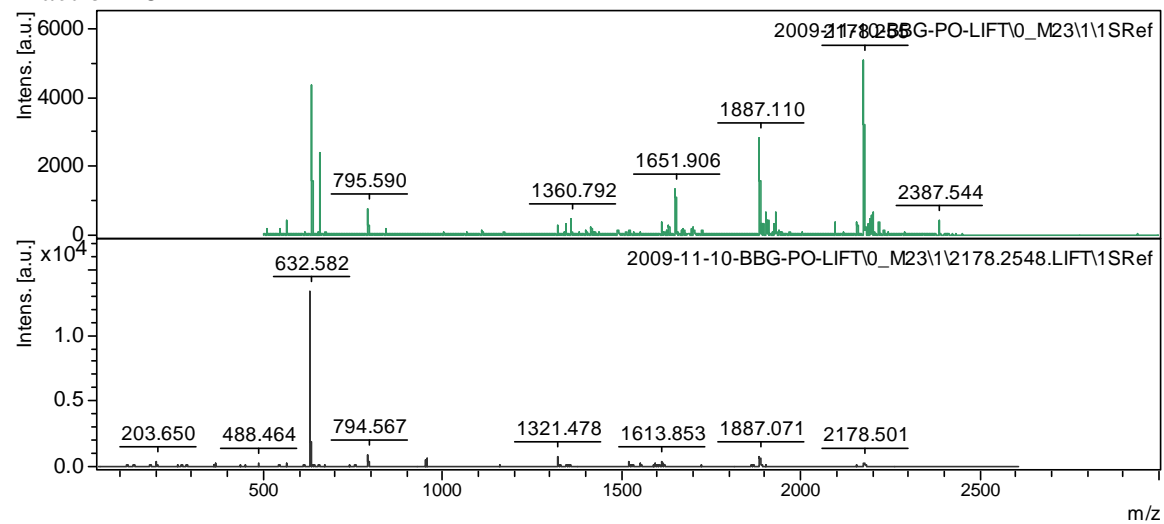
Fraction 26



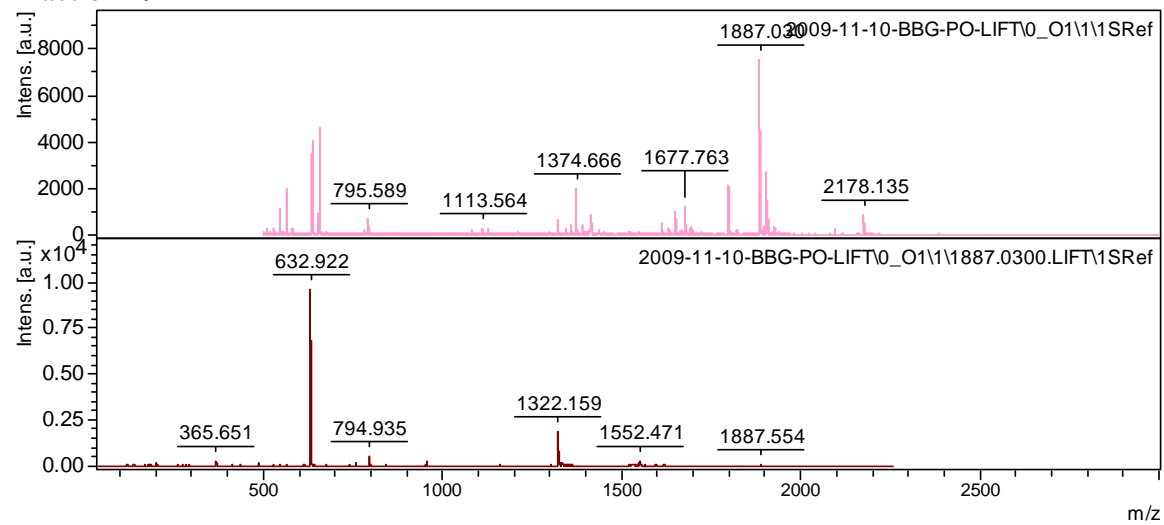
Fraction 27



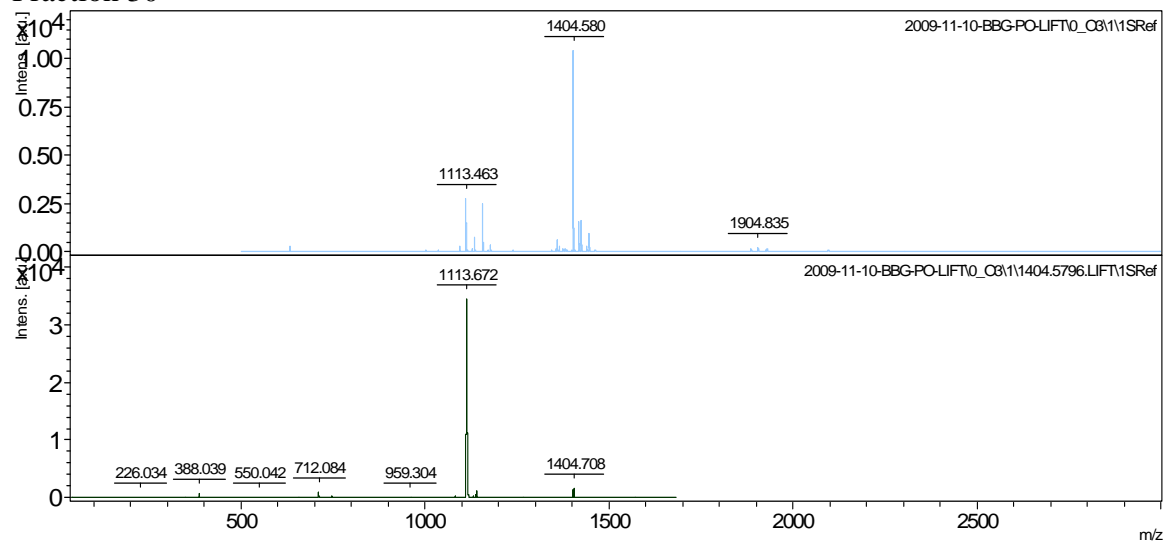
Fraction 28



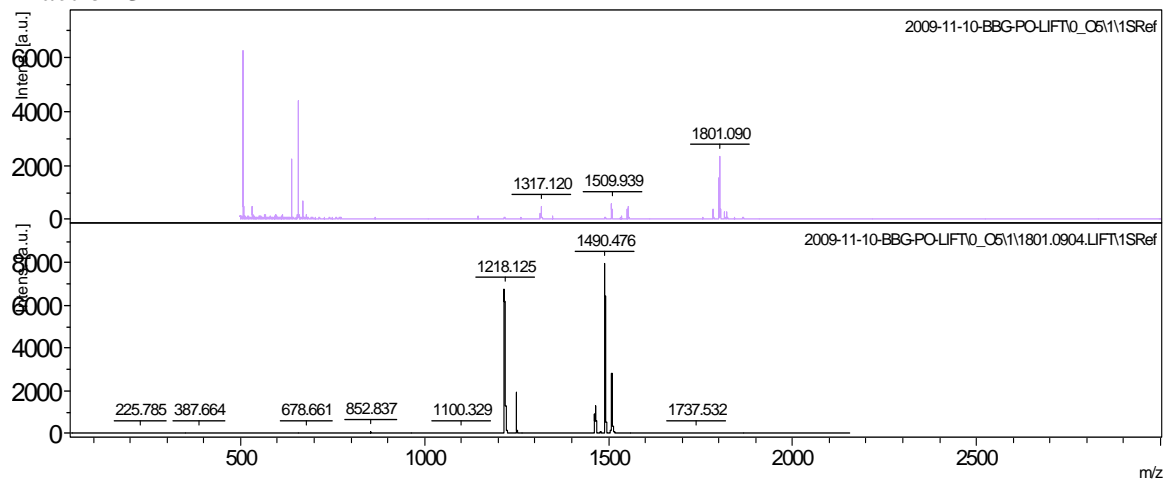
Fraction 29



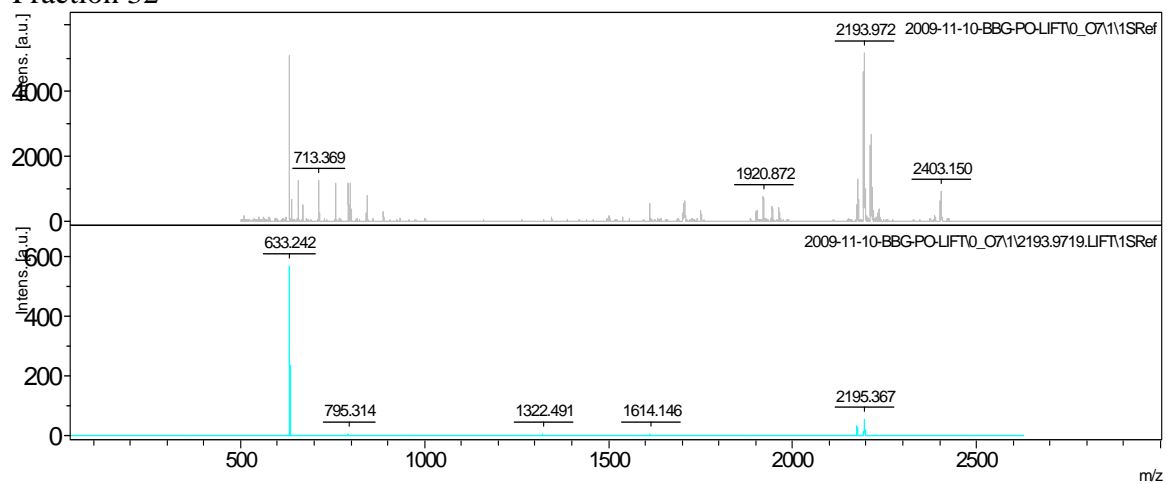
Fraction 30



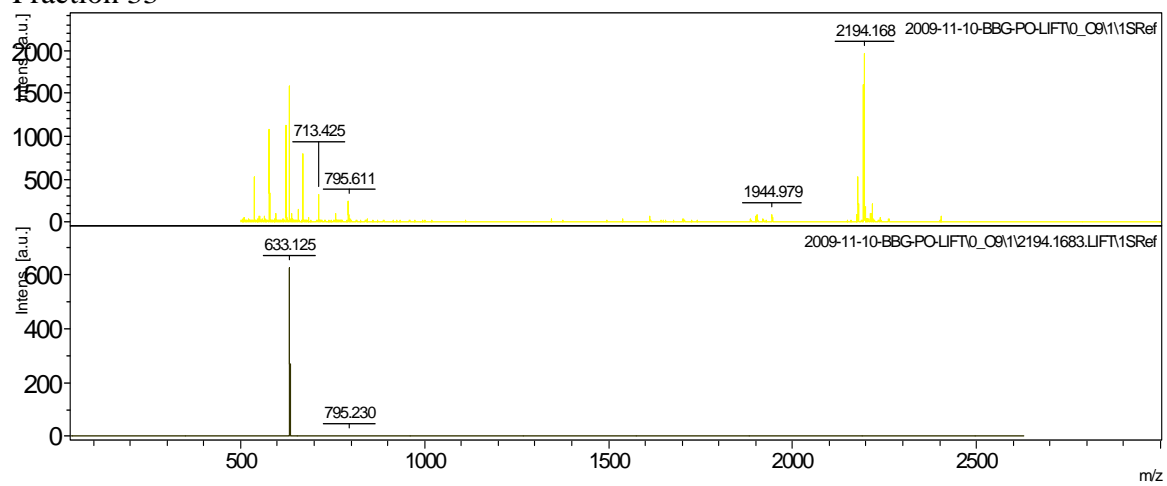
Fraction 31



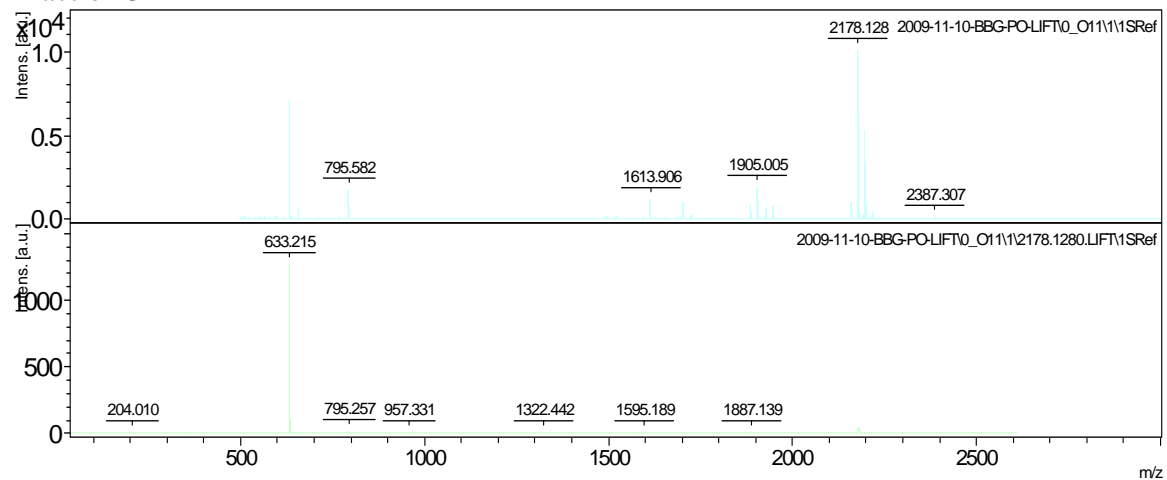
Fraction 32



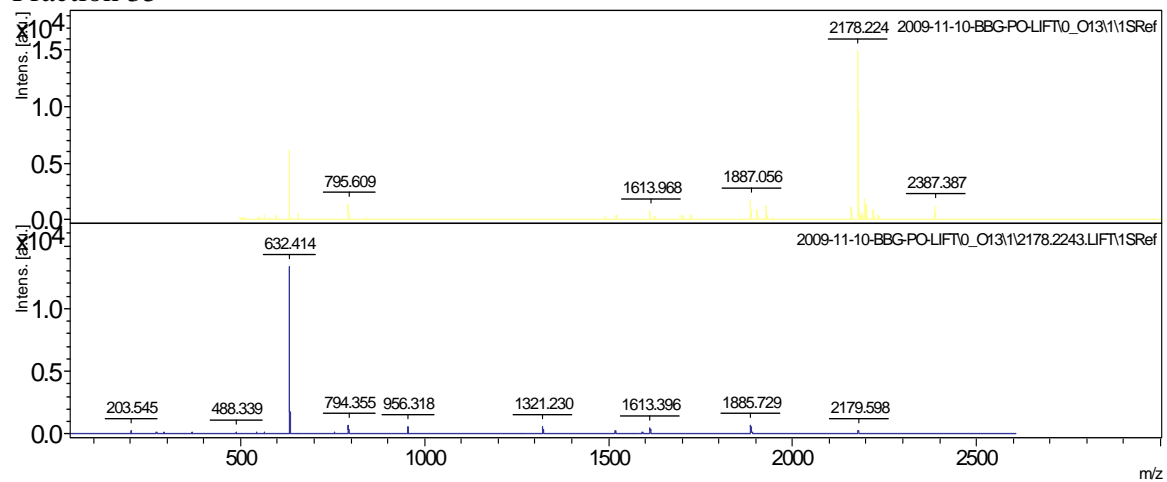
Fraction 33



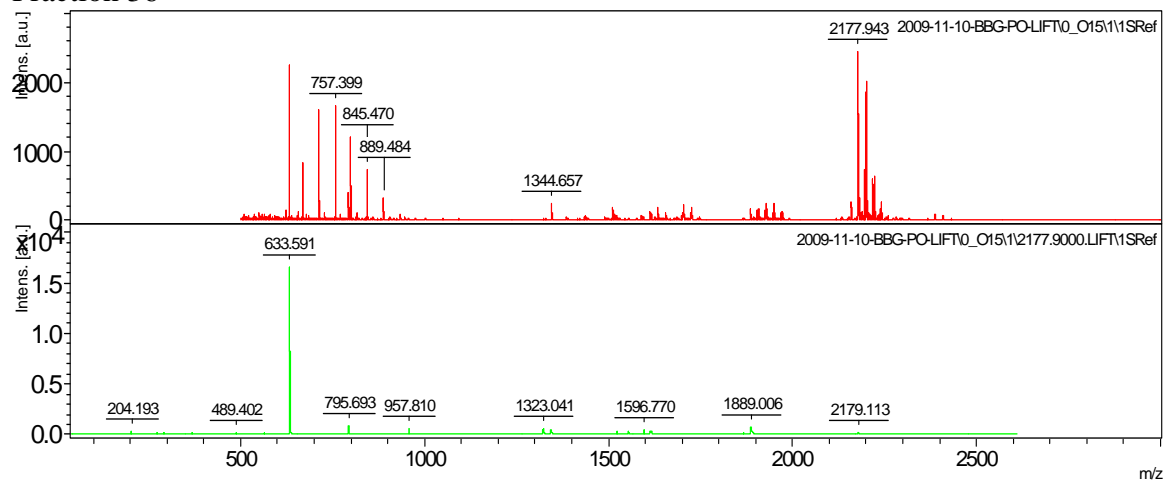
Fraction 34



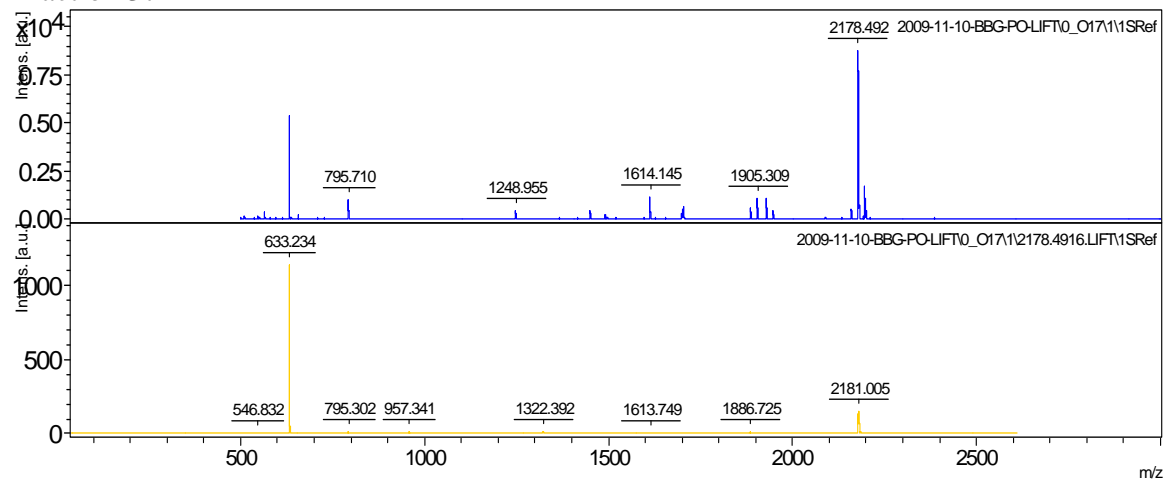
Fraction 35



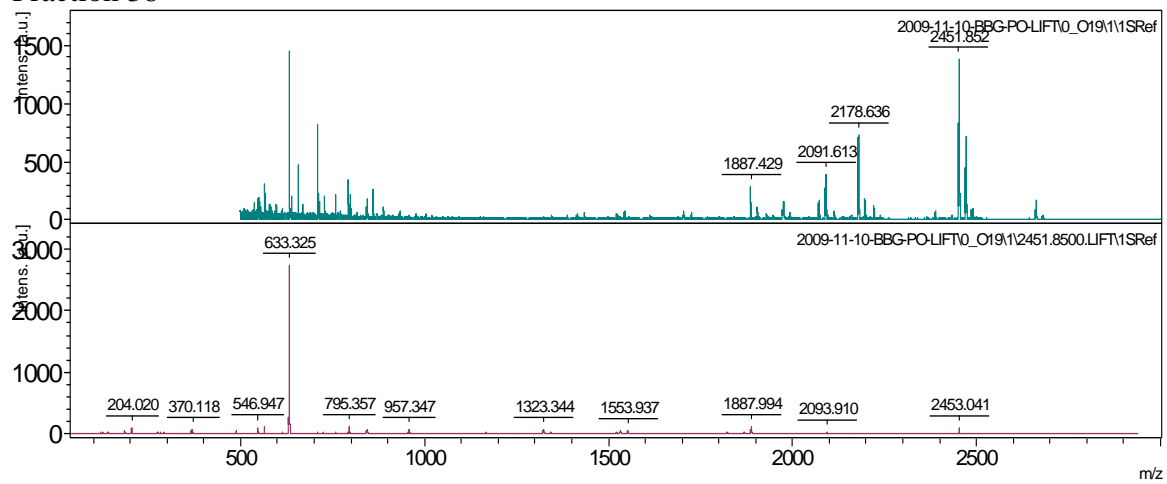
Fraction 36



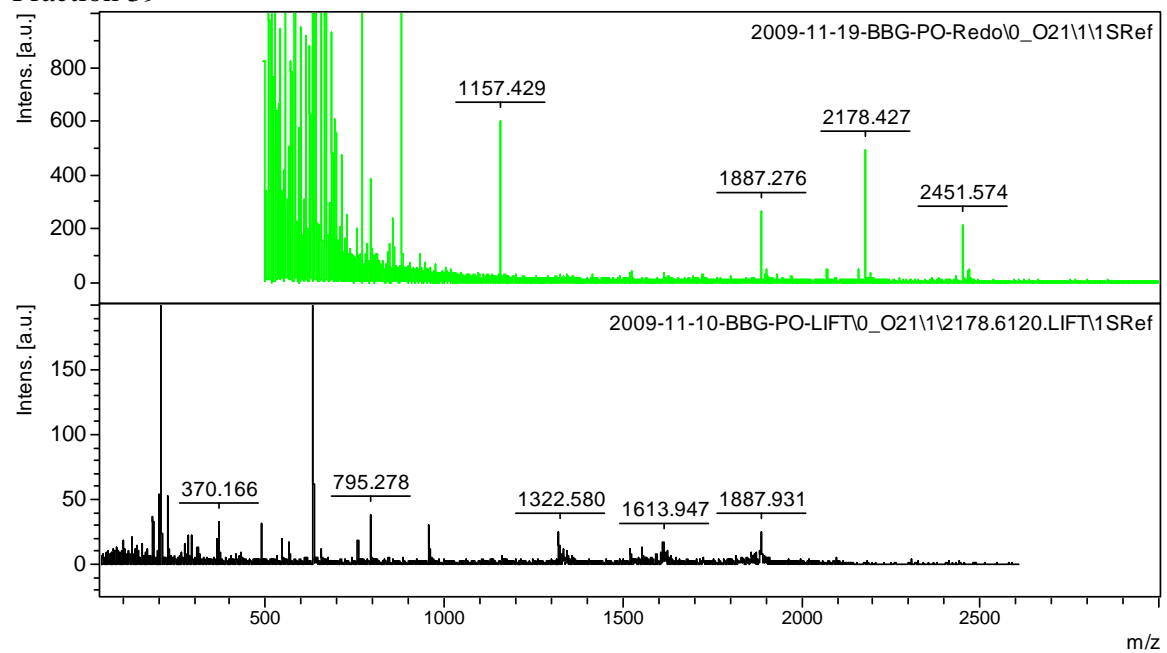
Fraction 37



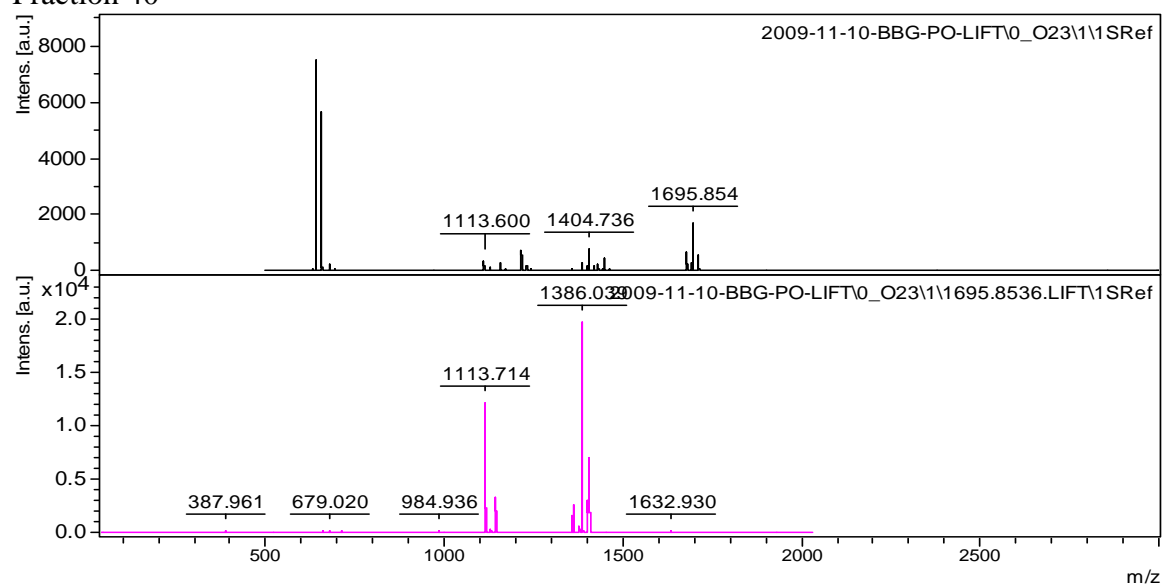
Fraction 38



Fraction 39



Fraction 40



Supplementary Table 2. Raw data of antibody binding from control and Lyme disease patient sera.

(a) IgG response of sera from Lyme disease patients on the BBG-AOAB microarray. Average = average of 4 median RFU values.

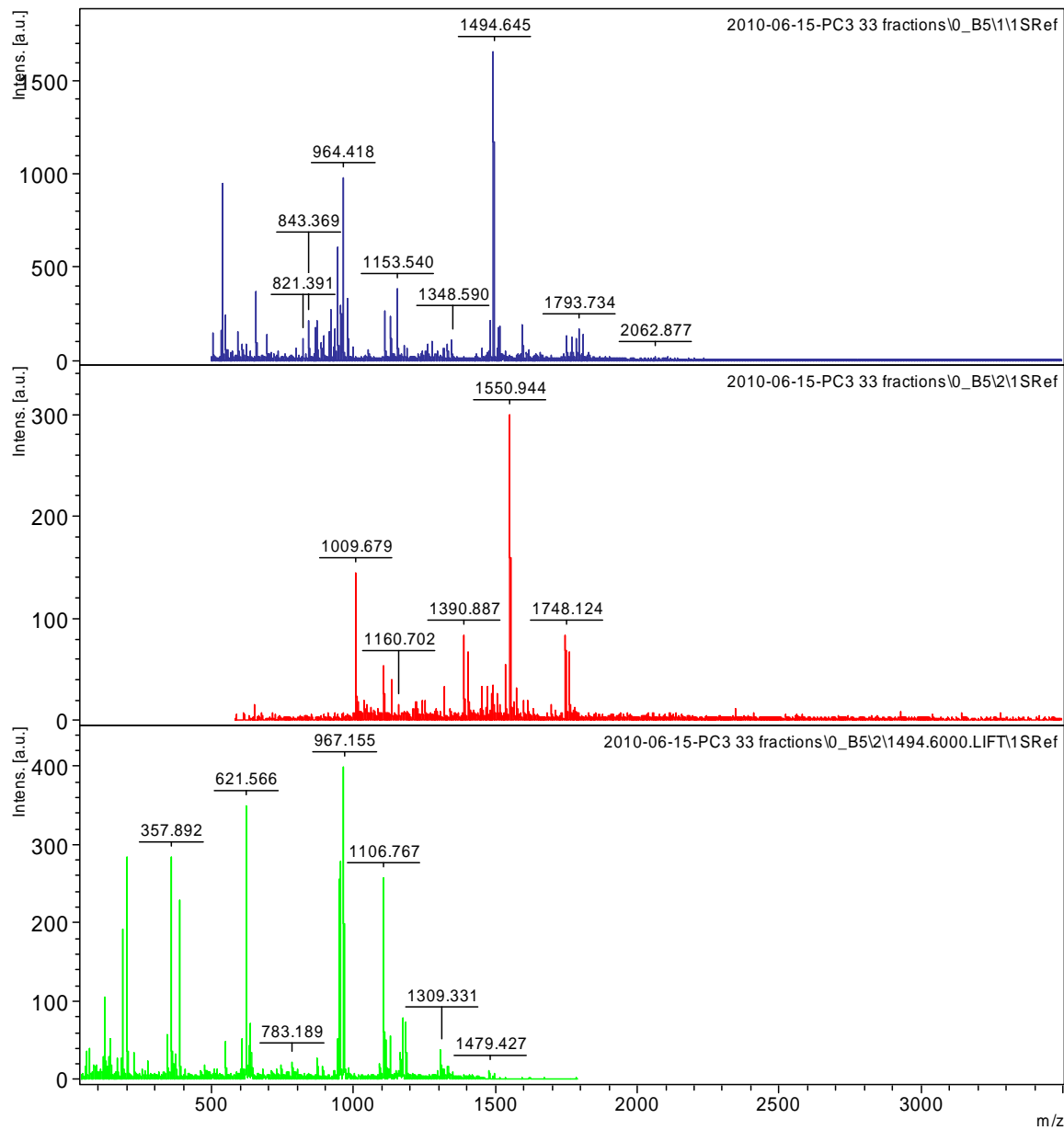
	PATIENT #1			PATIENT #2			PATIENT #3			PATIENT #4			PATIENT #5			PATIENT #6			PATIENT #7			PATIENT #8			PATIENT #9			PATIENT #10		
Chart ID	Average	STDEV	%CV	Average	STDEV	%CV	Average	STDEV	%CV	Average	STDEV	%CV	Average	STDEV	%CV	Average	STDEV	%CV	Average	STDEV	%CV	Average	STDEV	%CV	Average	STDEV	%CV			
1	1153	145	13	247	58	23	549	50	9	398	212	53	-152	498	-329	191	218	114	111	13	12	84	24	29	204	64	31	91	33	36
2	696	114	16	510	17	3	245	49	20	140	31	22	256	35	13	233	28	12	111	32	29	146	33	22	179	16	9	-7	94	-1340
3	1275	146	11	436	21	5	515	152	30	414	259	62	-117	474	-405	260	104	40	192	47	24	-113	154	-136	403	59	15	288	65	23
4	421	167	40	143	11	7	129	104	81	74	1	1	25	14	56	258	48	19	80	19	24	198	173	88	80	104	131	234	63	27
5	55	26	48	63	62	98	79	46	59	101	40	39	580	62	11	239	15	6	125	24	19	-31	60	-191	104	11	11	51	41	80
6	-8	29	-352	52	40	77	4	44	1108	29	3	10	247	5	2	223	79	35	140	68	49	69	19	28	-7	10	-150	41	31	76
7	727	197	27	230	42	18	118	32	27	487	183	38	342	245	72	196	93	48	48	16	34	80	109	136	-68	128	-188	32	40	127
8	358	45	13	62	8	14	73	18	25	7	7	100	68	51	75	290	113	39	19	10	53	-1	29	-5798	204	296	145	12	32	270
9	988	149	15	345	43	13	473	90	19	686	51	7	34	16	46	294	42	14	92	25	27	90	61	68	104	112	107	334	73	22
10	144	101	70	157	44	28	116	79	68	320	98	31	286	6	2	150	78	52	76	12	16	98	39	40	98	13	14	48	37	77
11	-31	58	-188	131	50	39	-5	273	-5198	175	40	23	-52	287	-551	136	47	34	63	6	10	83	73	88	64	170	266	14	6	40
12	7595	1809	24	1031	216	21	7242	1374	19	3170	325	10	97	202	207	626	92	15	140	38	27	690	65	9	-132	189	-143	2164	272	13
13	-33	299	-898	46	9	19	51	13	26	95	19	20	170	67	39	20	33	169	46	60	130	47	18	39	67	51	76	19	23	123
14	44	177	407	124	81	65	44	1	3	9	12	133	62	36	59	124	118	95	-52	7	-13	-32	60	-190	-38	168	-441	-30	54	-180
15	-40	41	-101	134	40	30	83	49	59	64	55	86	278	35	13	139	11	8	93	56	60	-6	52	-905	148	43	29	-16	154	-960
16	182	72	40	58	13	23	125	57	45	54	55	101	574	130	23	58	18	31	76	22	29	46	94	206	97	18	19	50	80	158
17	2238	296	13	774	35	5	609	127	21	574	233	41	109	44	41	130	94	73	373	88	24	369	69	19	-51	234	-459	476	23	5
18	-126	100	-80	357	79	22	237	111	47	238	8	4	320	152	48	89	11	13	158	42	26	194	26	14	55	52	95	213	20	9
19	-17	184	-1069	57	33	57	139	97	70	140	23	16	78	65	83	158	18	12	-18	94	-511	71	23	32	186	46	25	-52	29	-56
20	142	12	8	111	38	35	43	60	141	51	77	151	167	153	92	126	62	49	44	1	2	101	22	22	-137	183	-134	54	88	162
21	196	46	23	98	16	16	8	15	182	-4	9	-223	129	74	57	68	70	104	137	48	35	93	34	36	-46	63	-137	32	14	44
22	114	51	45	61	12	19	-29	56	-195	54	24	45	461	106	23	-29	100	-343	36	15	42	-64	55	-87	39	11	29	-69	55	-80
23	40	138	349	227	55	24	38	31	80	128	2	2	-131	238	-182	57	107	189	-55	52	-95	-103	142	-138	188	107	57	47	63	135
24	364	424	116	218	14	6	-16	86	-523	60	90	152	487	315	65	241	33	14	155	36	23	123	18	15	-3	53	-1630	75	18	24
25	266	53	20	186	42	22	43	28	65	160	47	30	-4	48	-1197	272	44	16	40	58	144	-20	41	-205	127	33	26	-66	97	-148
26	167	285	170	685	226	33	1839	395	21	1017	209	21	752	36	5	591	165	28	313	30	9	770	269	35	98	267	274	861	180	21
27	-36	49	-136	237	67	28	261	59	23	177	12	7	312	118	38	179	112	63	17	32	183	-23	8	-36	193	148	77	52	34	65
28	115	45	39	253	71	28	116	28	24	49	12	25	-132	735	-557	334	169	51	19	45	238	353	27	8	90	45	50	17	16	92
29	304	33	11	146	48	33	237	67	28	6	10	150	331	73	22	44	70	158	10	37	368	-38	22	-59	32	69	217	-31	58	-191
30	132	34	25	214	23	11	97	16	16	24	3	13	1163	179	15	103	13	12	-28	51	-182	124	30	24	238	112	47	92	7	7
31	-8	104	-1304	113	29	26	61	40	66	31	38	122	-75	474	-630	138	20	14	34	30	88	-70	64	-92	77	22	29	53	43	82
32	214	68	32	69	4	6	91	26	29	11	4	34	221	112	51	134	88	65	-15	60	-391	49	79	162	-4	197	-4927	8	14	168
33	2781	146	5	1276	336	26	2539	587	23	1232	302	25	824	199	24	435	105	24	722	33	5	1157	172	15	807	127	16	1020	222	22
34	228	34	15	230	42	18	39	101	263	111	28	25	15	53	366	55	60	108	91	33	36	50	9	19	-6	146	-2546	77	31	41
35	250	91	37	325	50	15	-21	28	-136	246	94	38	32	339	1072	323	81	25	99	16	16	169	48	28	274	78	29	195	34	18
36	557	62	11	126	109	86	147	40	28	85	57	68	238	316	133	162	183	113	32	38	119	185	44	24	96	70	73	63	56	89
37	-50	124	-249	4	9	202	83	20	25	23	25	108	400	175	44	291	145	50	-3	37	-1242	-1	11	-2132	-63	74	-117	-19	58	-300
38	-3	79	-2637	32	16	52	-36	34	-96	26	40	152	-43	435	-1024	234	84	36	67	29	43	-46	99	-215	41	12	30	21	111	539
39	469	139	30	728	205	28	148	28	19	560	120	21	495	100	20	429	203	47	126	35	28	279	31	11	195	49	25	635	169	27
40	529	125	24	341	257	75	463	109	24	112	144	129	2681	940	35	698	311	45	205	48	23	470	116	25	585	103	18	698	124	18
41	991	164	17	206	37	18	160	33	21	193	81	42	-220	324	-148	188	43	23	11	4	39	195	57	29	-71	61	-85	59	12	21
42	1001	337	34	138	40	29	143	16	11	145	59	41	525	336	64	209	41	19	0	24	-7202	285	59	21	54	25	46	44	15	33
43	131	33	25	50	11	21	43	74	171	46	12	27	1465	234	16	0	11	-3208	67	24	36	-128	84	-66	-96	145	-152	2	25	1050
44	863	129	15	326	66	20	162	26	16	93	50	54	714	204	29	160	91	57	197	24	12	305	75	25	245	100	41	423	105	2

(b) IgG response of control sera on the BBG-AOAB microarray. Average = average of 4 median RFU values.

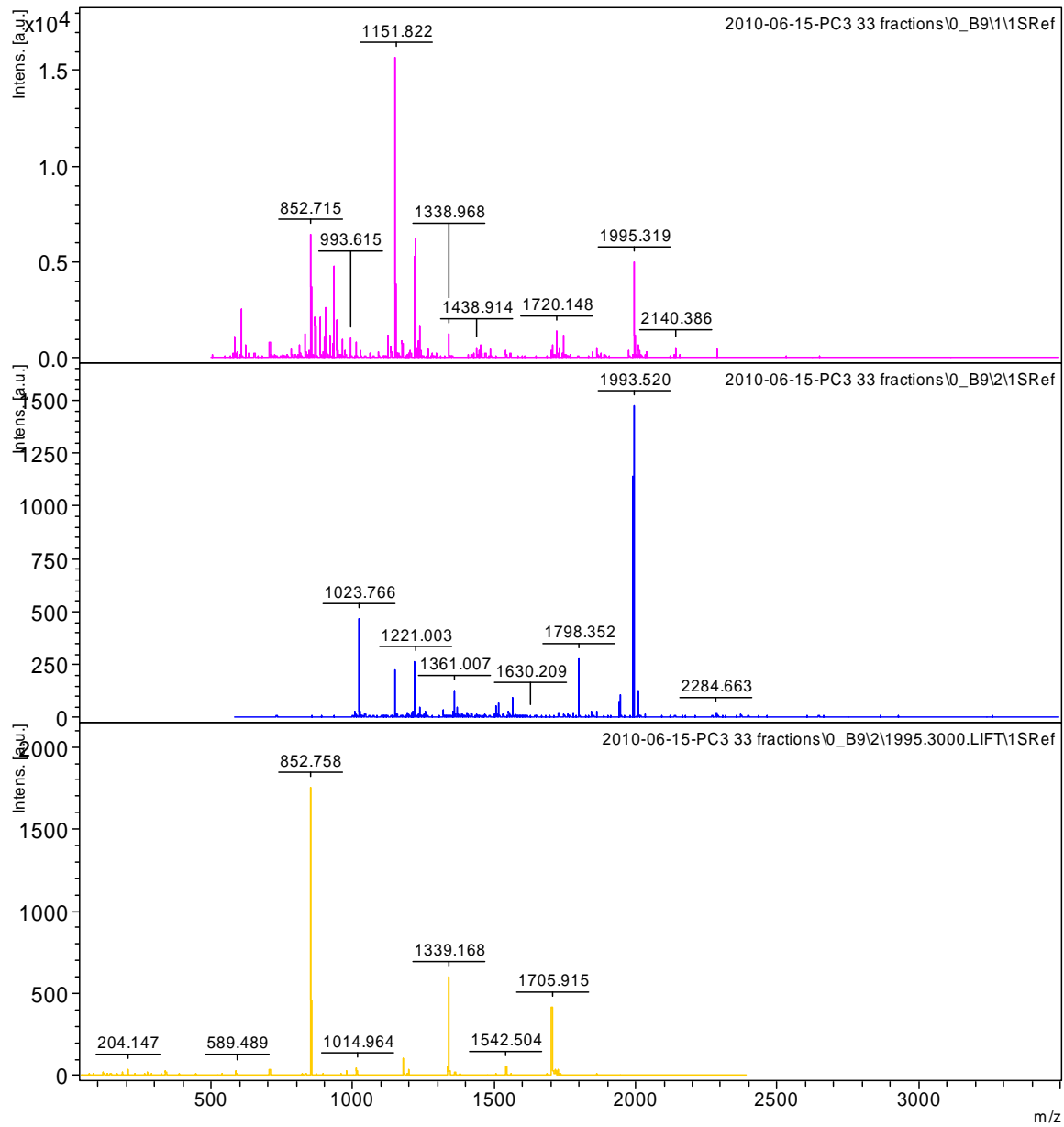
	CONTROL #1			CONTROL #2			CONTROL #3			CONTROL #4			CONTROL #5			CONTROL #6			CONTROL #7			CONTROL #8		
Chart ID	Average	STDEV	%CV	Average	STDEV	%CV	Average	STDEV	%CV	Average	STDEV	%CV	Average	STDEV	%CV	Average	STDEV	%CV	Average	STDEV	%CV	Average	STDEV	%CV
1	373	257	69	-5	34	-716	-152	31	-355	191	3	22	111	17	59	84	8	42	21	4	20	49	6	13
2	322	71	22	92	62	67	256	48	35	233	2	9	111	10	12	146	4	16	19	6	30	47	8	17
3	-151	435	-289	17	6	36	-117	35	29	260	5	15	192	10	11	-113	9	29	37	7	17	179	42	23
4	149	221	148	7	11	162	25	17	25	258	13	85	80	19	43	198	6	35	22	9	41	84	15	18
5	0	29	-8779	43	16	36	580	20	29	239	1	11	125	15	-196	-31	9	36	13	3	20	44	12	27
6	12	14	118	19	2	12	247	35	462	223	3	24	140	24	-4760	69	3	21	17	5	31	26	11	42
7	303	87	29	19	1	5	342	12	12	196	5	26	48	16	31	80	3	14	14	1	7	48	38	79
8	284	105	37	11	16	141	68	244	-2122	290	5	21	19	25	3703	-1	3	21	11	1	13	50	18	36
9	676	291	43	7	12	167	34	4	5	294	4	20	92	9	15	90	13	34	21	5	22	68	5	8
10	190	115	61	32	7	22	286	46	42	150	4	27	76	7	18	98	0	0	12	5	41	47	11	23
11	-42	122	-295	20	4	18	-52	102	-1388	136	2	10	63	7	13	83	7	22	17	2	14	56	11	20
12	-67	134	-202	61	7	11	97	40	32	626	9	30	140	36	22	690	17	24	41	10	23	111	50	45
13	-15	21	-140	61	5	9	170	30	31	20	4	28	46	0	0	47	10	31	13	0	0	24	9	39
14	53	38	72	41	42	103	62	5	9	124	3	22	-52	7	39	-32	1	4	14	1	10	20	4	18
15	-16	85	-522	21	14	67	278	67	-256	139	10	55	93	8	35	-6	4	25	12	1	12	35	1	4
16	-8	68	-821	54	30	56	574	37	-64	58	2	21	76	15	72	46	13	78	11	2	17	16	8	49
17	866	169	20	66	18	27	109	13	12	130	9	26	373	22	18	369	7	12	39	7	18	106	19	17
18	286	87	30	47	20	43	320	56	35	89	7	42	158	12	18	194	8	27	20	1	6	59	11	18
19	54	76	141	27	2	8	78	20	50	158	4	17	-18	7	47	71	7	29	19	2	8	50	2	3
20	237	62	26	29	31	106	167	22	43	126	5	30	44	6	21	101	3	11	14	4	26	33	4	13
21	21	5	25	29	15	51	129	61	-574	68	4	27	137	10	-104	93	4	25	17	3	20	24	1	4
22	17	4	20	5	14	304	461	28	-704	-29	3	22	36	8	87	-64	13	53	15	4	28	22	1	3
23	109	92	84	46	14	30	-131	1	1	57	3	27	-55	5	14	-103	4	28	14	6	47	18	12	66
24	312	319	102	13	13	99	487	94	-568	241	3	29	155	40	-269	123	3	9	14	3	18	33	7	22
25	134	32	24	7	5	76	-4	4	21	272	2	23	40	16	77	-20	5	15	17	7	43	11	3	24
26	405	180	44	121	1	1	752	289	25	591	21	35	313	57	66	770	12	12	117	26	23	104	10	10
27	937	86	9	29	17	59	312	79	88	179	5	26	17	9	25	-23	9	53	22	4	18	50	10	20
28	332	115	35	25	13	54	-132	38	34	334	5	28	19	13	42	353	8	20	22	4	21	23	8	35
29	31	12	38	10	19	191	331	32	41	44	8	55	10	17	77	-38	3	11	11	1	13	23	0	0
30	-456	284	-62	7	5	71	1163	25	20	103	8	38	-28	12	21	124	7	17	15	2	15	42	7	17
31	-138	146	-106	1	12	889	-75	43	-445	138	4	19	34	20	50	-70	9	49	21	4	20	16	3	18
32	218	39	18	13	14	108	221	2	2	134	7	31	-15	18	87	49	1	9	16	4	23	33	9	26
33	1866	251	13	221	37	17	824	45	15	435	49	24	722	85	25	1157	2	1	159	33	21	241	60	25
34	55	103	188	27	10	37	15	63	26	55	3	13	91	30	160	50	7	23	24	5	21	52	13	25
35	-95	128	-135	9	28	310	32	11	5	323	6	17	99	23	33	169	3	17	22	4	20	29	9	32
36	-18	221	-1225	29	29	97	238	12	9	162	5	37	32	31	38	185	5	12	22	3	11	19	17	89
37	-21	52	-243	28	4	12	400	116	157	291	2	9	-3	17	50	-1	8	41	18	2	12	8	13	157
38	108	38	35	60	2	3	-43	233	129	234	7	15	67	6	17	-46	18	129	50	11	23	26	28	106
39	753	331	44	38	33	87	495	195	38	429	27	66	126	9	10	279	3	7	51	2	4	59	11	19
40	99	91	92	144	25	17	2681	173	57	698	12	24	205	12	8	470	25	19	57	5	9	89	18	20
41	-68	95	-140	76	30	39	-220	60	16	188	16	47	11	7	18	195	11	28	21	2	9	41	7	17
42	-64	146	-228	56	33	59	525	44	8	209	6	15	0	4	6	285	16	-466	38	11	29	36	10	28
43	-360	303	-84	13	11	87	1465	44	69	0	11	84	67	43	202	-128	6	182	14	3	20	16	6	35
44	224	166	74	66	17	25	714	93	17	160	0	0	197	60	38	305	49	113	37	12	32	93	23	25

Supplementary Table 3. MALDI-TOF MS and MS/MS data of the 10 peaks collected from C18 HPLC separation of PC3 cell GSL-AOABs. For each fraction, MS at positive mode, MS at negative mode and MS/MS at positive mode were obtained and shown below.

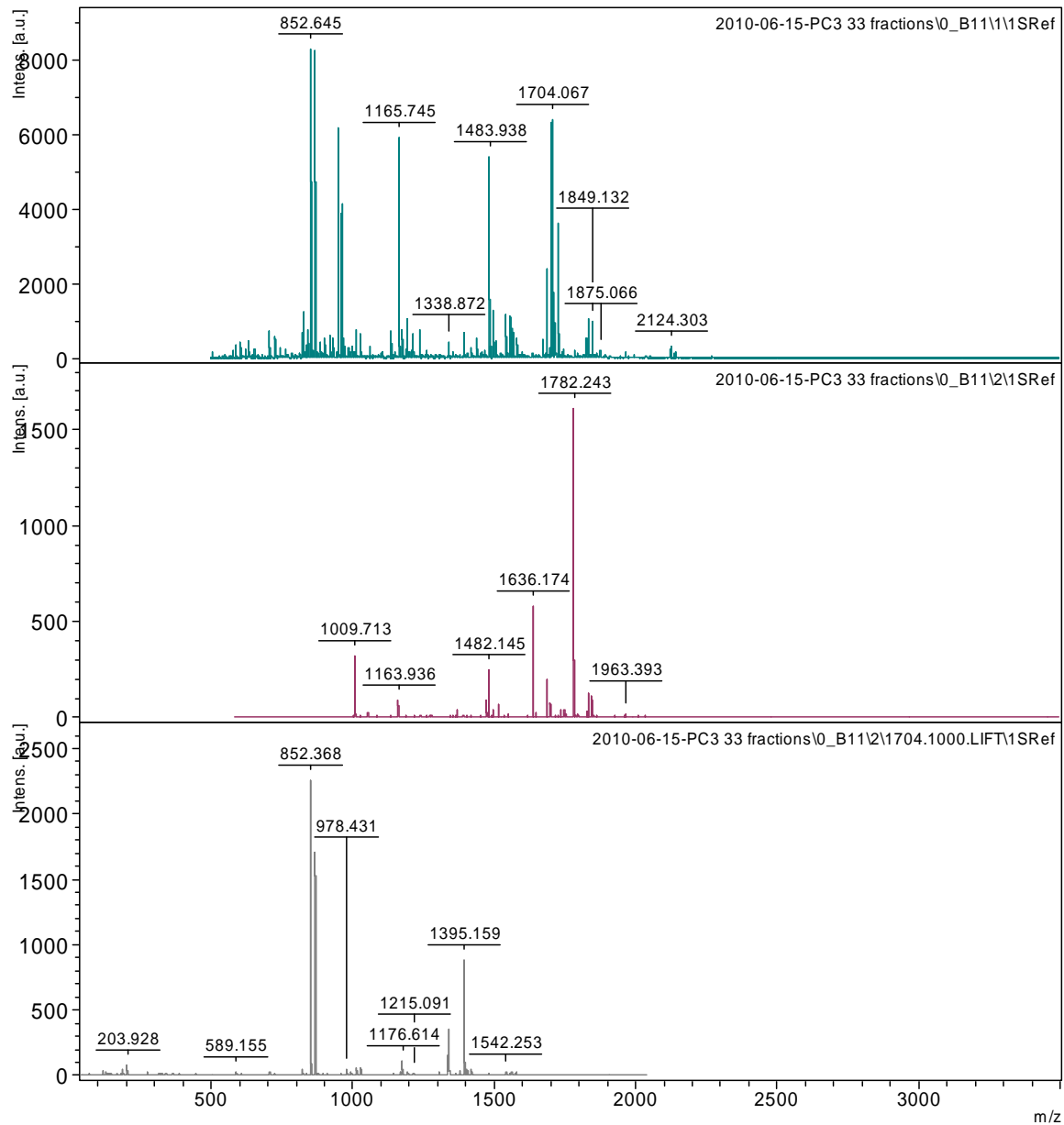
Fraction 3



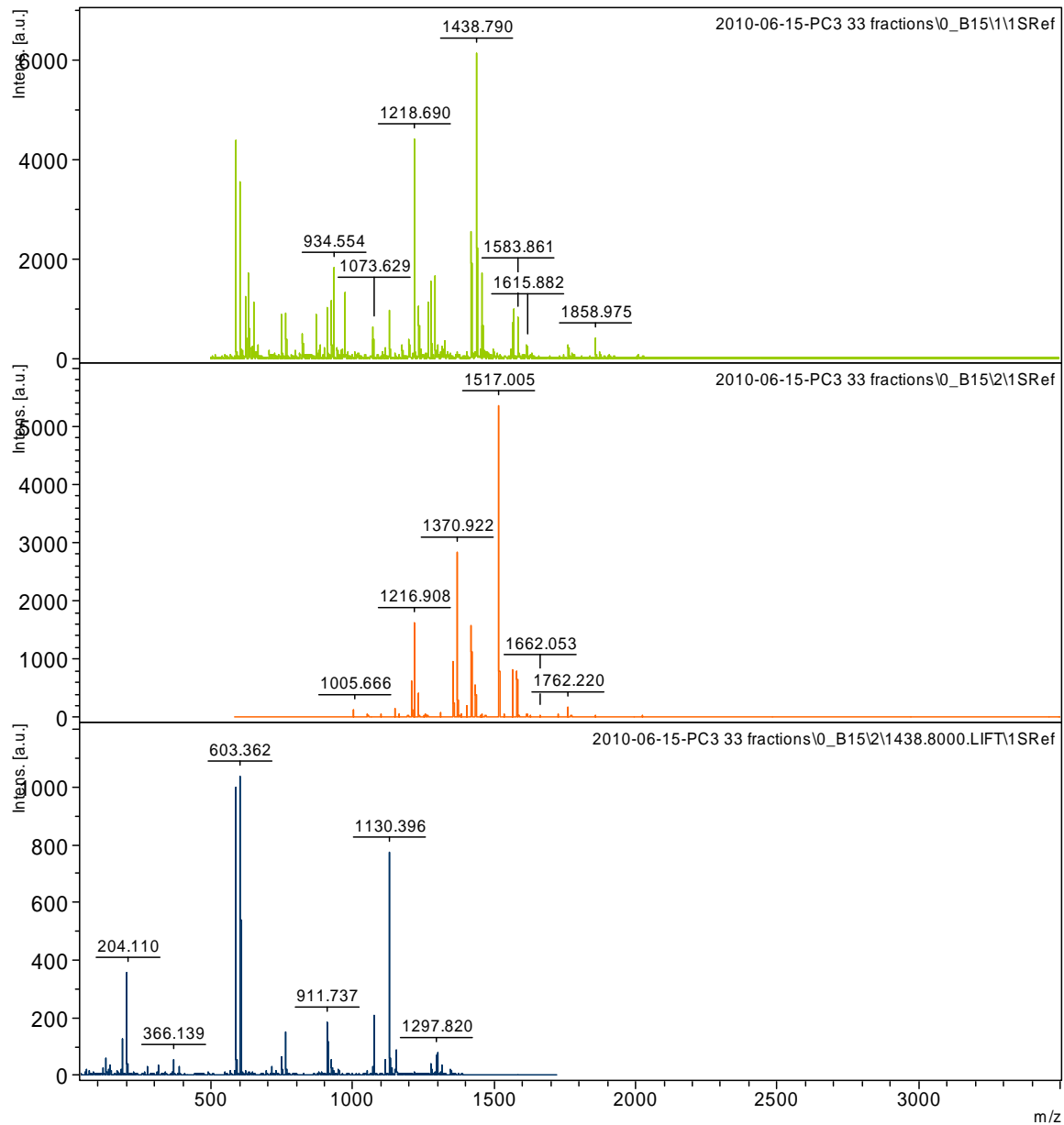
Fraction 5



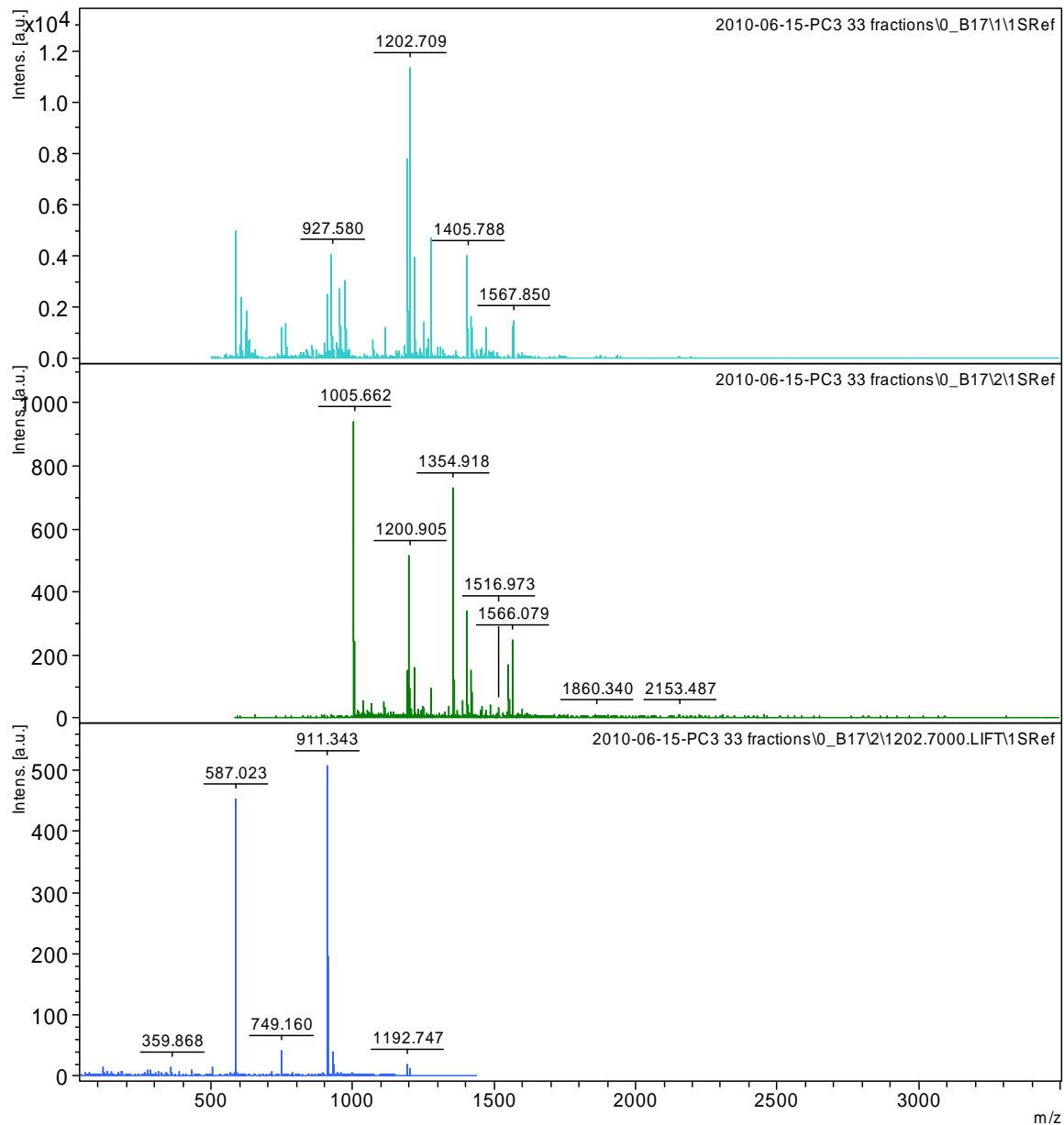
Fraction 6



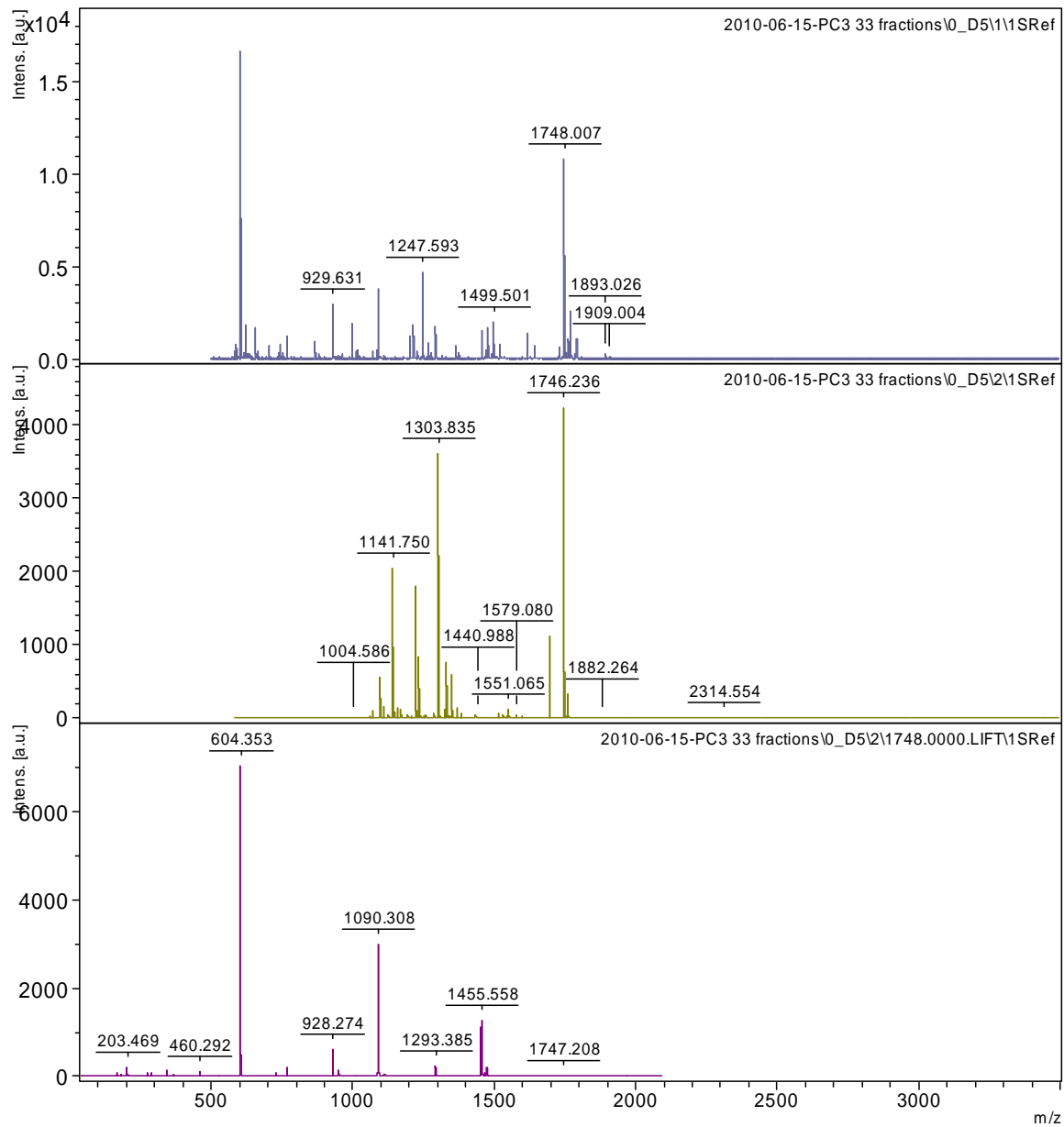
Fraction 8



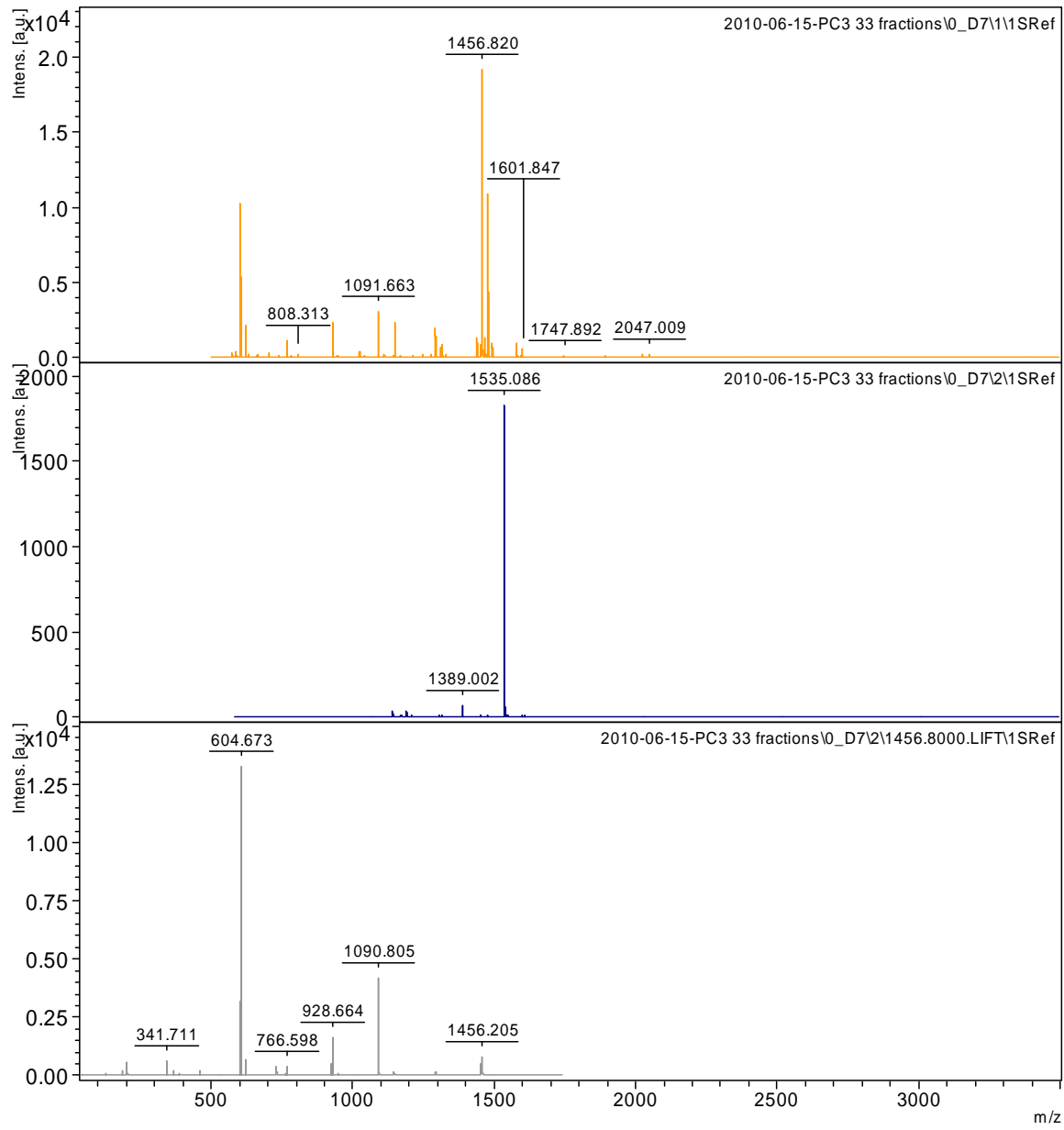
Fraction 9



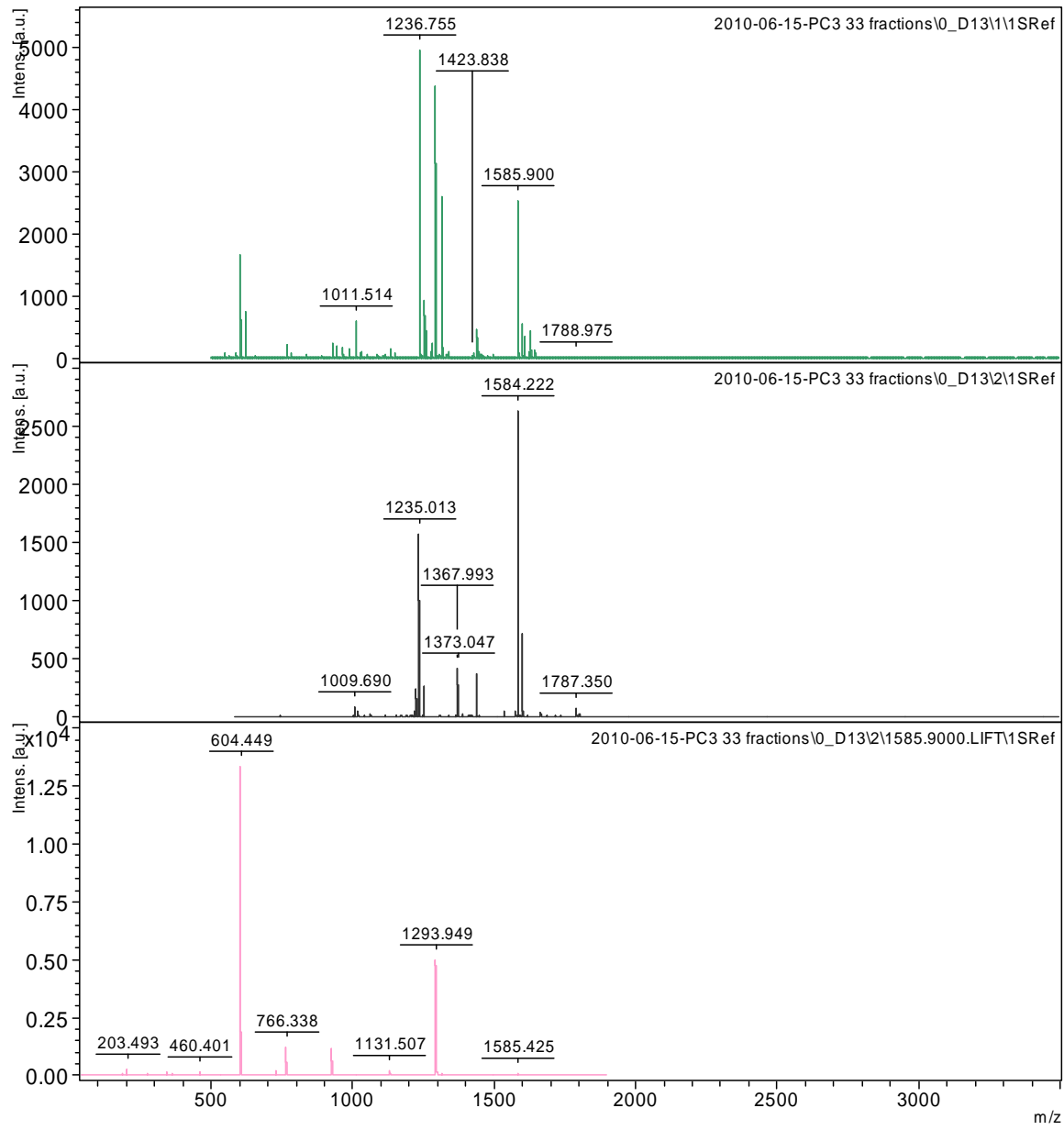
Fraction 15



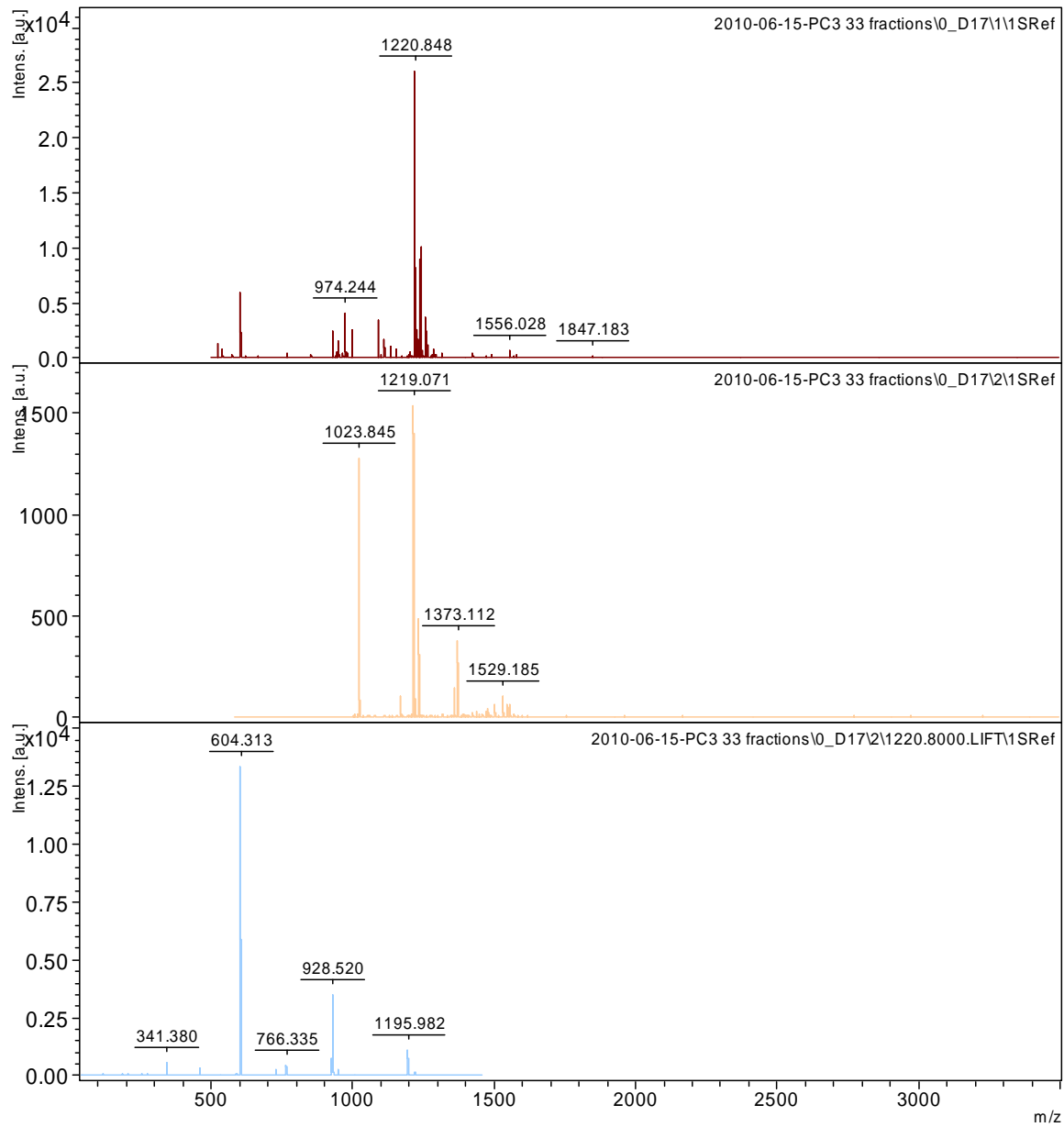
Fraction 16



Fraction 18



Fraction 20



Fraction 21

